



Published in final edited form as:

Nat Rev Clin Oncol. 2021 January ; 18(1): 35–55. doi:10.1038/s41571-020-0408-9.

ROS1-dependent cancers — biology, diagnostics and therapeutics

Alexander Drilon^{1,2,✉}, Chelsea Jenkins³, Sudarshan Iyer³, Adam Schoenfeld^{1,2}, Clare Keddy³, Monika A. Davare^{3,✉}

¹Early Drug Development and Thoracic Oncology Service, Division of Solid Tumor Oncology, Department of Medicine, Memorial Sloan Kettering Cancer Center, New York, NY, USA.

²Department of Medicine, Weill Cornell Medical College, New York, NY, USA.

³Department of Pediatrics, Oregon Health & Science University, Portland, OR, USA.

Abstract

The proto-oncogene *ROS1* encodes a receptor tyrosine kinase with an unknown physiological role in humans. Somatic chromosomal fusions involving *ROS1* produce chimeric oncoproteins that drive a diverse range of cancers in adult and paediatric patients. ROS1-directed tyrosine kinase inhibitors (TKIs) are therapeutically active against these cancers, although only early-generation multikinase inhibitors have been granted regulatory approval, specifically for the treatment of *ROS1* fusion-positive non-small-cell lung cancers; histology-agnostic approvals have yet to be granted. Intrinsic or extrinsic mechanisms of resistance to ROS1 TKIs can emerge in patients. Potential factors that influence resistance acquisition include the subcellular localization of the particular ROS1 oncoprotein and the TKI properties such as the preferential kinase conformation engaged and the spectrum of targets beyond ROS1. Importantly, the polyclonal nature of resistance remains underexplored. Higher-affinity next-generation ROS1 TKIs developed to have improved

✉ drilon@mskcc.org; davarem@ohsu.edu.

Author contributions

All authors researched the data for the article. A.D., C.K. and M.A.D. made substantial contributions to discussions of content. A.D., C.J., S.I., A.S. and M.A.D. wrote the manuscript, and A.D. and M.A.D. reviewed/edited the manuscript before submission.

Competing interests

A.D. has received honoraria from or participated on the advisory boards of 14ner/Elevation Oncology, Abbvie, ArcherDX, AstraZeneca, Beigene, BergenBio, Blueprint Medicines, Exelixis, Helsinn, Hengrui Therapeutics, Ignyta/Genentech/Roche, Loxo/Bayer/Lilly, Monopteros, MORE Health, Pfizer, Remedica, Takeda/Ariad/Millennium, TP Therapeutics, Tyra Biosciences and Verastem; research support paid to his institution from Exelixis, GlaxoSmithKlein, Pfizer, PharmaMar, Taiho and Teva; research support from Foundation Medicine; personal fees from Boehringer Ingelheim, Merck, Merus and Puma; and CME honoraria from Axis, Medscape, OncLive, Paradigm Medical Communications, Peerview Institute, PeerVoice, Physicians Education Resources, Research to Practice, Targeted Oncology and WebMD. The other authors declare no competing interests.

Peer review information

Nature Reviews Clinical Oncology thanks Myung-Ju Ahn, Luc Friboulet, who co-reviewed with Francesco Facchinetti, Justin Gainor and the other, anonymous, reviewer(s) for their contribution to the peer review of this work.

Supplementary information

Supplementary information is available for this paper at <https://doi.org/10.1038/s41571-020-0408-9>.

RELATED LINKS

cBioPortal: <https://www.cbioportal.org/>

Chimera: <https://www.cgl.ucsf.edu/chimera/>

GTex Portal: <https://gtexportal.org/home/>

MatchMaker: <https://www.cgl.ucsf.edu/chimera/docs/ContributedSoftware/matchmaker/matchmaker.html>

RCSB PDB 3ZBF: <https://www.rcsb.org/structure/3ZBF>

intracranial activity and to mitigate ROS1-intrinsic resistance mechanisms have demonstrated clinical efficacy in these regards, thus highlighting the utility of sequential ROS1 TKI therapy. Selective ROS1 inhibitors have yet to be developed, and thus the specific adverse effects of ROS1 inhibition cannot be deconvoluted from the toxicity profiles of the available multikinase inhibitors. Herein, we discuss the non-malignant and malignant biology of ROS1, the diagnostic challenges that *ROS1* fusions present and the strategies to target ROS1 fusion proteins in both treatment-naive and acquired-resistance settings.

The first *ROS1* gene fusion was identified in the U118MG glioblastoma cell line in 1987 (REFS¹⁻³). Subsequently, the oncogenic potential of this fusion (*FIG-ROS*, now called *GOPC-ROS1*) in gliomagenesis and the signalling pathways that it activates were characterized in a series of elegant studies⁴⁻⁶. In 2007, an unbiased phospho-tyrosine proteomic screen revealed *ROS1* fusions in a small subset of non-small-cell lung cancers (NSCLCs)⁷. Diverse *ROS1* fusions have since been identified across various cancer types occurring in adults and/or children.

The clinical activity of ROS1-directed tyrosine kinase inhibitors (TKIs) was first prospectively explored in patients with NSCLC. The kinase domains of ALK and ROS1 share ~70% homology and adopt similar conformations when inhibited by the ALK, ROS1 and MET TKI crizotinib; therefore, an expansion cohort comprising patients with ROS1-rearranged NSCLC was added to the phase I PROFILE 1001 trial, in which the activity of crizotinib had previously been explored in patients with *ALK*-rearranged NSCLC⁸ (a cohort of patients with MET-dependent NSCLC would subsequently also be added to this trial). Substantial activity was observed in this expansion cohort⁸, leading to the FDA and EMA approvals of crizotinib for the treatment of advanced-stage *ROS1*-rearranged NSCLC in 2016.

Subsequently, other ROS1 TKIs entered clinical testing. The ROS1, TRK and ALK TKI entrectinib was approved by the FDA and by the Ministry of Health, Labour and Welfare of Japan⁹ for the treatment of *ROS1*-rearranged NSCLC in 2019 and 2020, respectively. Notably, the activity of entrectinib was concurrently explored in patients with other *ROS1* fusion-positive cancers using a histology-agnostic approach. In parallel, the discovery of ROS1-intrinsic mechanisms of resistance to crizotinib resulted in the rational design of next-generation ROS1 inhibitors to overcome this issue.

In this Review, we discuss ROS1 biology within the contexts of normal physiology and oncogenesis. We also describe the evolving science of molecularly targeted therapy for ROS1-dependent cancers.

ROS1 biology

ROS1 in non-malignant tissues

Evolutionary conservation.—The tyrosine kinase activity of ROS1 was first discovered in 1982 as the oncogenic component of the UR2 avian sarcoma retrovirus v-ros^{10,11}. Specifically, p68^{gag-ros} (also known as v-ros) was found to have tyrosine kinase activity, was homologous to transforming proteins of other retroviruses known at the time (such as

v-src, v-yes, v-erbB, v-fgr and v-abl), and robustly transformed chicken embryo fibroblasts and neuroretinal cells^{10–14}. Hybridization studies combining *v-ros* complementary DNA with human placental genomic DNA led to the cloning of the gene encoding cellular ROS (*c-ROS*), a receptor tyrosine kinase (RTK)¹⁵. Subsequent years saw the cloning of *c-ROS* complementary DNA from other vertebrates and invertebrates as well as from human cancer cells^{3,16,17}. Although previously known as *c-ROS* or *ROS*, *ROS1* is now the standardized gene name. Analyses have confirmed that *ROS1* encodes an evolutionarily conserved RTK that is phylogenetically related to the well-characterized *Drosophila melanogaster* protein sevenless (encoded by *sev*) and the *Caenorhabditis elegans* protein roller-3 (*rol-3*)¹⁸.

Structure.—The *ROS1* gene is located on chromosome 6 (region 6q22.1) and generates two dominant splice variants of ROS1 encoded by either 43 or 44 exons (FIG. 1a). Shorter ROS1 isoforms with unknown functional relevance have also been identified¹⁹. Exons 1–34 encode the largest extracellular N-terminal domain of any protein within the human RTK family. Structurally unique among human RTKs, this extracellular domain is composed of nine fibronectin type III repeats and three β -propeller domains²⁰. Deduced by homology to other RTKs, the N-terminal region of ROS1 is connected to intracellular tyrosine kinase and C-terminal domains via a single transmembrane domain (FIG. 1b). Considerable homology exists between the tyrosine kinase domains of mammalian ROS1 and members of the insulin receptor family of RTKs, particularly ALK^{21,22}.

Signalling.—In June 2020, Kiyozumi et al.²³ discovered that the extracellular domain of the mouse ROS1 receptor binds to neural epidermal growth factor–like like 2 (NELL2), a testicular germ cell-secreted lumicrine factor. Functional activation of human ROS1 receptor via NELL2 can be presumed from these studies in mice but remains to be tested; additional or alternate ligands or co-receptors in human tissues or organs other than the testes cannot be ruled out at this stage. The cellular signalling pathways that are coupled to ROS1 catalytic activation have largely been extrapolated from experiments with oncogenic ROS1 fusion proteins that lack most of the ROS1 extracellular domains, UR2 virus v-ros, or chimeric receptor constructs (such as TRK–ROS1 or EGFR–ROS1) stimulated with their cognate ligands^{4,6,24–28}. Evidence from these studies indicates that ROS1 activation results in autophosphorylation of specific tyrosine residues in the intracellular domain that serve as docking sites for various adaptor proteins. The recruitment of SH2 domain-containing and other canonical adaptor proteins stimulates signalling via the RAS–RAF–MEK–ERK, PI3K–AKT–mTOR and JAK–STAT3 pathways, which broadly regulate cell survival, growth and proliferation^{4,6,18,25,28} (FIG. 1c). Non-receptor tyrosine phosphatases, including SHP1 and SHP2, also interact with and are substrates of ROS1. SHP2 is a pleiotropic signalling protein²⁹ and is probably an important transducer of ROS1 signalling during normal physiological development as well as tissue physiology and oncogenesis. By contrast, SHP1 dephosphorylates ROS1 and thereby downregulates effector pathway activation by this RTK²⁴.

ROS1 in cancer

Overexpression.—A variety of cancers aberrantly express ROS1. Initially, 30–56% of primary brain tumours, including low-grade gliomas, glioblastomas and meningiomas, were

reported to express ROS1 (REFS^{30–33}) secondary to promoter demethylation³⁴. However, transcriptomic analyses included in The Cancer Genome Atlas and the Ivy Glioblastoma Atlas projects subsequently showed that deregulated ROS1 expression occurs in only 0.5–1% of glioblastomas^{35–38}. ROS1 overexpression is observed in 80–100% of metastatic oral squamous cell carcinomas and has been functionally linked to an invasive disease phenotype in one study³⁹. In mouse models of *Kras*-mutant lung cancer, expression of *Ros1* is upregulated, suggesting that ROS1 and RAS signalling can cooperate in tumorigenesis^{40,41}. Finally, ROS1 is upregulated in E-cadherin-deficient breast cancers, and ROS1 inhibition has a synthetic lethal effect in preclinical models of these cancers⁴². The ongoing phase II ROLO trial of crizotinib plus fulvestrant in patients with E-cadherin-negative, oestrogen receptor (ER)-positive lobular breast cancer⁴³ was designed on the basis of these findings.

Splice variants.—Systematic reverse transcription PCR (RT-PCR) and *ROS1* 5′ sequence analyses identified aberrant expression of six fetal *ROS1* transcripts in NSCLC specimens⁴⁴. Five of these splice variants have exon skipping in the extracellular N-terminal region, with four resulting in frameshifts that produce premature stop codons and thus truncated protein isoforms containing only extracellular sequences of variable lengths. The four isoforms lacking the catalytic domain probably function similarly to secreted EGFR splice variants (soluble EGFR), which contain only the extracellular domain and operate in a dominant-negative manner; these variants lacking the kinase domain are unlikely to support tumorigenesis⁴⁵. However, computational algorithms predict that alternate translation start sites downstream of a newly gained stop codon exist in exons 21, 23 and 30. Translation from these sites might generate novel N-terminally truncated, kinase domain-containing, constitutively active ROS1 variants.

Mutation and amplification.—Examination of the tumour genome sequencing datasets curated in the cBioPortal^{46,47} reveals numerous missense mutations in *ROS1* that do not cluster in a particular domain of the protein. These mutations are currently variants of unknown significance. By contrast, *ROS1* kinase domain mutations are crucial mediators of the resistance of *ROS1* fusion-positive cancers to ROS1 TKIs (as discussed later relevance of these amplifications as predictive biomarker in this Review). Data from the cBioPortal also remains unknown. Indeed, functional studies on the *ROS1* amplifications in several tumour types, including effects of *ROS1* amplification or mutation (in cancers breast cancers and soft-tissue sarcomas, although the without *ROS1* fusions) on pathogenesis are lacking.

ROS1 fusions *Fusion biology*

Partner diversity and structure.—At least 55 different 5′ gene partners have been identified in fusion with the 3′ regions of *ROS1* (FIG. 2a, Supplementary Table 1). Considerable interpatient partner-gene heterogeneity has been observed in adult glioblastomas, paediatric gliomas, NSCLCs, Spitzoid neoplasms and in inflammatory myofibroblastic tumours (IMTs). Furthermore, the frequency of individual fusion partners varies between cancer types (FIG. 2b), which probably reflects variations in the intrinsic levels of genome stability, susceptible loci and transcriptional activation of upstream partner genes in the cell of origin. In NSCLCs, *CD74-ROS1* is the most common *ROS1* fusion (~44%), followed by *EZR-ROS1* (16%), *SDC4-ROS1* (14%) and *SLC34A2-ROS1* (10%)

(FIG. 2b). By contrast, *GOPC-ROS1* is the most common (~75%) *ROS1* fusion in adult glioblastoma, and the spectrum of fusion partners is narrower in this malignancy. Similarly, *GOPC* is the only *ROS1* fusion partner identified in cholangiocarcinomas to date^{48,49}.

ROS1 fusions are formed via intrachromosomal or interchromosomal mechanisms. In adult glioblastomas, *ROS1* fusions arise largely through intrachromosomal 6q microdeletions⁵⁰, whereas the majority of recurrent *ROS1* fusions in NSCLCs result from interchromosomal translocations^{8,51–58} (Supplementary Table 1). These observations suggest that differences in chromatin architecture or dynamics exist between tumour types. The common structural theme of functional *ROS1* fusions is the loss of the majority of the *ROS1* extracellular domain and in-frame fusion of the N-terminal portion of a partner gene with the intracellular kinase domain-containing region of *ROS1* (FIG. 2c).

Oncogenesis.—In contrast to *ROS1* overexpression, splice variants, mutations or amplifications, a wealth of data support the notion that *ROS1* fusions are bona fide drivers of oncogenesis^{4,6,50,59–63}. *ROS1* fusions exhibit ligand-independent, constitutive catalytic activity. These fusions activate canonical cell survival and growth signalling pathways, including the aforementioned RAS–MEK–ERK, JAK–STAT3, PI3K–AKT–mTOR and SHP2 cascades. The subcellular localization conferred by the 5′ fusion partner (FIG. 2d) seems to influence downstream signalling. Endosome-localized *ROS1* fusions (*SDC4-ROS1* and *SLC34A2-ROS1*) have a greater capacity to activate the MAPK (ERK) signalling pathway than the endoplasmic reticulum-localized fusion *CD74-ROS1* despite the fact that all three fusions activate STAT3 signalling to a similar extent⁶². Regardless, all activating *ROS1* fusions tested to date induce neoplastic transformation of cells in vitro and in vivo in animal models^{4,6,48,57,60}. For example, transgenic mice expressing *CD74-ROS1*, *SDC4-ROS1* or *EZR-ROS1* in *Tp53* wild-type, type II alveolar cells develop numerous lung adenomas and adenocarcinomas⁶⁴.

The co-occurrence of *ROS1* fusions with other oncogenic alterations has been observed^{54,65}; however, *ROS1* fusions tend to be mutually exclusive with other driver mutations⁶⁶, including *ALK*, *RET* and *NTRK* fusions in NSCLCs, IMTs^{67,68} and Spitzoid neoplasms⁶⁹, *FGFR2* and *IDH* alterations in cholangiocarcinomas⁷⁰, and *EGFR*, *IDH* and *PDGFRA* alterations in gliomas⁷¹. *ROS1* fusions alone are sufficient to induce tumorigenesis in model systems, although cooperation with other aberrant oncogene or tumour suppressor pathways can promote disease that is more aggressive. In a genetically engineered mouse model of glioblastoma, for example, combining dual deletion of p16^{INK4a} and p19^{ARF} (both of which are encoded by *Cdkn2a*) with *GOPC-ROS1* expression results in highly aggressive tumours with a reduced latency and increased penetrance compared with expression of *GOPC-ROS1* alone⁶. Additionally, loss of *CDKN2A* and *CDKN2B* or aberrations that activate PI3K–mTOR signalling (for example, *PTEN* loss-of-function mutations) co-occur in most *ROS1*-rearranged glioblastomas in adult patients^{6,50}. Finally, concurrent expression of *Kras*^{G12D} and *GOPC-ROS1* increases lung metastasis in a mouse model of cholangiocarcinoma relative to that observed with either oncogene alone⁶¹.

Clinicopathological features

Associated tumour types.—*ROS1* fusions have been identified in 22 diverse adult and paediatric malignancies (Supplementary Table 1) at variable frequencies (including some only identified in a single patient to date). Larger cohort studies have revealed that *ROS1* rearrangement occurs recurrently in a subset of cancers, including NSCLC (1–2%) and gastrointestinal cancers (including 1–9% of cholangiocarcinomas)^{48,49} as well as in less common cancers such as Spitzoid neoplasms (17%), IMTs (10%), gliomas (0.5–1%) and anaplastic large cell lymphomas⁶³ (4%) (FIG. 2a, Supplementary Table 1). Thus, *ROS1* fusions seem to have transformative propensities in cells of different lineages, including cells of epithelial, astroglial, neuroendocrine and mesenchymal origin.

ROS1 fusion-positive NSCLCs are the most common of these cancers owing to the high incidence of NSCLCs in general. In NSCLCs, *ROS1* fusions occur predominantly in lung adenocarcinomas in younger (median age of 50 years) never smokers (~80%)^{72–74}. Interestingly, *ROS1*-rearranged NSCLCs are associated with a higher rate of venous thromboembolism⁷⁵ than that observed in unselected patients with NSCLCs⁷⁶ or in those with tumours harbouring other oncogenic drivers⁷⁷. Mechanistically, cancer-related mucins that are present extracellularly and/or intracellularly in signet-ring cells⁷⁸ within *ROS1* fusion-positive tumours potentially ligate P-selectin and/or L-selectin, which can activate platelets and subsequent embolization⁷⁹.

The clinicopathological features of other *ROS1* fusion-positive cancers are less well defined. *ROS1* fusion-positive gliomas, many of which are identified in children, can be low or high grade^{71,80,81}. *ROS1*-rearranged IMTs, which also predominantly occur in children, are mainly found in the lungs and/or abdomen and have a fascicular spindle cell growth pattern⁶⁷. *ROS1*-rearranged Spitzoid tumours, which have no distinguishing histopathological features, are observed in both adult and paediatric patients⁸².

Responsiveness to chemotherapy.—The activity of chemotherapy has been systematically studied in patients with *ROS1* fusion-positive NSCLCs (Supplementary Table 2). Pemetrexed, as monotherapy or in combination with a platinum-based agent (with or without bevacizumab), was predominantly used in these studies; objective response rates (ORRs) of 45–60% and median progression-free survival (PFS) durations of 5–23 months were observed with such treatments^{56,83–90}. In the first-line setting, the median PFS durations were longer with pemetrexed-based versus non-pemetrexed-based chemotherapy^{88,90}. Notably, pemetrexed-based chemotherapy is more active in patients with *ROS1* fusion-positive NSCLC than in those with *ROS1* wild-type NSCLC or NSCLCs harbouring other drivers (such as *KRAS* mutations). In one study⁸³, the ORR was 58% and the median PFS duration was 77.5 months among patients with *ROS1* fusion-positive NSCLC, compared with 30% and <6 months, respectively, for patients with *EGFR*-mutant, *EML4-ALK* fusion-positive or *ROS1*, *EGFR*, *ALK* and *KRAS* wild-type NSCLCs. Low levels of thymidylate synthase mRNA in *ROS1* fusion-positive cancers (relative to *ROS1* wild-type cancers) might underlie this benefit from pemetrexed. Indeed, even among *ROS1* fusion-positive NSCLCs, lower thymidylate synthase mRNA levels were associated with increased PFS (184 days versus 110 days in patients with low versus high levels of

thymidylate synthase mRNA)⁹⁰. Counterintuitively, thymidylate synthase protein levels, as determined by immunohistochemistry (IHC) H-s core, were not associated with PFS in another series, although only 18 patient samples were analysed⁸³.

Immune-checkpoint inhibition.—The immunophenotype of *ROS1* fusion-positive NSCLC has been described in multiple reports^{91–93}. Among ten patients across three studies, three had a PD-L1 tumour proportion score of 0%, four of 1–49% and three of 50%^{91–93}. Tumour mutational burdens are generally low (0–5 mutations per megabase) across fusion-positive cancers⁹⁴, although tumour mutational burden has not been characterized in a large series of *ROS1* fusion-positive cancers thus far. Seven patients with *ROS1* fusion-positive NSCLCs included in the Immunotarget registry were treated with single-agent immune-checkpoint inhibitors (ICIs); five of these patients had progressive disease, one had an objective response and data were missing for the remaining patient (median PFS was not estimated)⁹³. *ROS1* TKIs or pemetrexed-based chemotherapy should thus be considered prior to single-agent ICI in patients with *ROS1*-rearranged NSCLC. The activity of chemoimmunotherapy combinations (for example, platinum, pemetrexed and pembrolizumab) in patients with *ROS1* fusion-positive cancers has not yet been described.

Molecular diagnostics

Single-gene assays.—*ROS1* fusions can be detected using several tests, none of which is without limitations^{95,96}. Fluorescence in situ hybridization (FISH) is predicated on the use of fluorescently labelled, paired ‘break apart’ probes that bind to the 5′ and 3′ ends of *ROS1*. A split 5′/3′ pattern of fluorescence or isolated 3′ signals in 15% of tumour cells constitutes a positive test⁷². The sensitivity and specificity of this approach is difficult to ascertain, largely because early studies used this assay as a diagnostic gold standard⁹⁷. Notably, false-positive results (non-functional fusions or those with isolated 3′ signals⁹⁸) and false-negative results (fusions with complex staining patterns or those formed by intrachromosomal microdeletions such as *GOPC–ROS1*) can occur⁹⁹, necessitating confirmation using alternative assays.

RT-PCR only enables the detection of specific fusions, which limits its use¹⁰⁰. The AmoyDx RT-PCR assay, which identifies select *ROS1* fusions involving *CD74*, *SLC34A2*, *SDC4*, *EZR*, *TPM3*, *LRIG3* or *GOPC*, was used as the diagnostic platform in a phase II trial of crizotinib for patients with *ROS1* fusion-positive NSCLC conducted in Asia¹⁰¹, resulting in its approval as a companion diagnostic for crizotinib in Taiwan, China, Japan and South Korea as well as in European Union certification¹⁰². The sensitivity and the specificity of this assay were 100% and 85%, respectively, in one series⁹⁷.

Next-generation sequencing.—Next-generation sequencing (NGS) can enable the detection of genomic alterations in up to hundreds of genes and can identify *ROS1* fusions, such as *GOPC–ROS1*, that are not detectable using FISH¹⁰³. Tumour DNA enrichment can be achieved through amplicon-based (for example, with Oncomine Dx Target Test) or hybrid capture-based approaches (as used in the FDA-approved FoundationOne CDx that has received pre-marketing authorization for *ROS1* fusion detection or the FDA-authorized MSK-IMPACT assay that has received New York State Department of Health validation for

ROS1 fusion detection). Hybrid capture is better suited to the detection of *ROS1* fusions, owing partly to the ability to interrogate broader regions of the genome and to better identify the fusion partner gene¹⁰⁴. NGS can be performed on tumour tissue-derived DNA or plasma circulating cell-free DNA (cfDNA). *ROS1* fusions have been detected through plasma cfDNA profiling¹⁰⁵, although this approach can be challenging owing to variations in disease extent, tumour location and DNA shedding rates that determine the concentration of tumour-derived DNA within the blood. Thus, the failure to detect a *ROS1* fusion in plasma cfDNA should prompt confirmatory tumour tissue-based sequencing, when feasible.

However, DNA-based NGS can fail to detect certain *ROS1* fusions owing to the inability to fully cover intronic breakpoints containing numerous repetitive elements. Targeted or whole-transcriptome RNA-based sequencing can overcome this limitation. In NSCLCs in which DNA-based NGS failed to detect an oncogenic driver, RNA-based anchored multiplex PCR using the ArcherDX assay (with FDA Breakthrough Device designation^{94,106}) identified actionable drivers in 14% of tumours, including *ROS1* fusions in 4%⁹⁴. Indeed, mRNA is used for the identification of gene fusions with Oncomine Dx, which is the only companion diagnostic test for *ROS1* fusions with FDA pre-market approval¹⁰⁷.

Immunohistochemistry.—IHC can be used as a screening tool for *ROS1* fusions¹⁰⁸: diffuse ROS1 staining of moderate to strong intensity is closely associated with the presence of a *ROS1* fusion¹⁰⁹. However, ROS1 staining patterns vary by fusion and antibody type (for example, D4D6 versus SP384)¹¹⁰. In one study, an H-score of 150 or the presence of 70% of cells with 2+ staining was determined as the optimal threshold for the IHC-based detection of *ROS1* fusions (using break-apart FISH as the gold standard), with similar levels of sensitivity and specificity observed with both the SP384 (93% and 100%, respectively) and D4D6 (91% and 100%, respectively)¹¹¹ antibodies. However, D4D6 yielded better accuracy in a separate study that used two cut-offs (including 1+ staining in any percentage of tumour cells)¹¹⁰. Unfortunately, test cut-offs are not standardized (for example, SP384 2+ staining in >30% of cells was used in another series)¹¹². Furthermore, non-neoplastic tissues, including reactive pulmonary epithelial proliferations, type II alveolar pneumocytes and osteoclast-type giant cells, can stain positive for ROS1 (REFS^{108,110}). Thus, although IHC can be used to screen for *ROS1* fusions in resource-challenged environments, nucleic acid-based testing should be considered for orthogonal confirmation in IHC-positive cases. In environments with sufficient payer coverage, DNA-based and/or RNA-based NGS should be considered as the primary testing modality.

ROS1 inhibitors

Binding modes

The ROS1 kinase domain exists in dynamic equilibrium between two main conformations that affect ATP and TKI binding. In the active, type I kinase conformation of ROS1, the phenylalanine of the aspartic acid–phenylalanine–glycine (DFG) motif immediately preceding the kinase domain activation loop is oriented into a hydrophobic pocket (‘DFG-in’ state) enabling access to the catalytic site and its coordination of magnesium and ATP binding. Most ROS1 TKIs, including crizotinib, entrectinib, ceritinib, ensartinib, brigatinib,

lorlatinib, repotrectinib and taletrectinib, are type I inhibitors that preferentially bind to the DFG-in conformations of their targets^{113–120}.

In the inactive, type II, ‘DFG-out’ kinase domain conformation, the DFG motif and activation loop are drawn towards the kinase surface to favour substrate obstruction and thus autoinhibition^{121,122}. The type II ROS1 inhibitors, such as cabozantinib and foretinib, bind favourably to the DFG-out conformation. While cabozantinib and foretinib are multikinase inhibitors, the rational design of novel type II inhibitors has the potential for greater selectivity than type I inhibitors because different kinases adopt less similar conformations in their inactive versus active states. Unfortunately, crystallographic structures of the DFG-out conformation are lacking for most kinases, hampering rational type II TKI discovery efforts.

Generations

Early-generation ROS1 TKIs (crizotinib, ceritinib and entrectinib) are clinically active, predominantly in patients with ROS TKI-naïve disease. For example, early clinical testing of entrectinib revealed that responses were not achieved in patients previously treated with ROS1 TKIs¹²³ (TABLE 1). Next-generation TKIs are defined in this Review as drugs that are clinically active against *ROS1* fusion-positive cancers following disease progression on an early-generation ROS1 TKI and, accordingly, have substantial intracranial activity (lorlatinib) and/or activity in the setting of recalcitrant *ROS1* kinase domain resistance mutations (such as repotrectinib and taletrectinib).

Spectrum of kinase inhibition

All ROS1 TKIs developed to date are multikinase inhibitors that can also inhibit ALK (crizotinib, ceritinib, entrectinib, ensartinib, brigatinib, lorlatinib and repotrectinib), TRKA, TRKB and/or TRKC (entrectinib, repotrectinib, taletrectinib and cabozantinib), MET (crizotinib and cabozantinib) and/or other kinases (such as EGFR, FLT3, SRC, JAK2, ACK, LTK and others) with equivalent or lower potency. Notably, not all ALK inhibitors can inhibit ROS1 (REF.¹²⁴). Modelling of alectinib in complex with DFG-in ALK revealed nuanced differences between the structures of ALK and ROS1 kinases, even in their type I states, thus explaining why alectinib does not effectively bind to ROS1 (REF.¹²⁴). These studies also showed that the type II inhibitor cabozantinib inhibits ROS1 but not ALK¹²⁴.

ROS1 inhibition in TKI-naïve cancers

Preclinical activity

The earliest studies examining the activity of crizotinib against *ROS1* fusions used the SLC34A2–ROS1-containing NSCLC cell line HCC78 (REFS^{72,100,125}), with more extensive investigations being hampered by the dearth of established cell lines or patient-derived xenograft models. Thus, most preclinical studies of ROS1 TKIs involved the transformed Ba/F3 CD74–ROS1 model^{119,120,124,126–130}. These cell-based dose–response assessments showed that crizotinib and brigatinib have equivalent inhibitory activity (half-maximal inhibitory concentration (IC₅₀) of 15.4 nM and 15.5 nM, respectively) and are approximately fourfold more potent inhibitors of cell growth than ceritinib (IC₅₀ 68 nM)

(Supplementary Figure 1). Entrectinib, foretinib and cabozantinib, with IC_{50} values of 2–6 nM, are more effective inhibitors of cell growth than crizotinib. The next-generation inhibitors lorlatinib, repotrectinib and taletrectinib are ~20–100-fold more effective than crizotinib for cell growth inhibition (IC_{50} 0.4 nM, 0.1 nM and 0.8 nM, respectively). Comprehensive comparisons of the activity of these inhibitors against different ROS1 fusions in a consistent isogenic cell-based model are lacking; however, anecdotal data suggest that early-generation and next-generation inhibitors each have modestly different in vitro activity in Ba/F3 cells expressing CD74–ROS1, GOPC–ROS1, EZR–ROS1, CEP85L–ROS1 or SLC34A2–ROS1 (REFS^{50,60,124,128,129}). Overall, preclinical efficacy is in the 0.1–75 nM range for all ROS1 TKIs; thus, these differences might not be meaningful in a clinical setting for drugs that achieve plasma concentrations well above the levels required for ROS1 inhibition (Supplementary Figure 1).

ROS1 inhibitors are active against *ROS1* fusion-containing cancers in animal models. Activity has been demonstrated with crizotinib in genetically engineered CD74–ROS1-driven and SDC4–ROS1-driven mouse models of lung adenocarcinoma¹³¹, foretinib in a GOPC–ROS1-driven mouse cholangiocarcinoma allograft model⁶⁰, entrectinib in a mouse Ba/F3 TEL–ROS1-driven allograft tumour model¹³², repotrectinib in a mouse Ba/F3 CD74–ROS1-driven allograft tumour model¹¹⁹ and taletrectinib in a patient-derived xenograft model of CD74–ROS1-driven NSCLC¹²⁰.

Clinical activity

NSCLC.—ROS1 TKI therapy is the current standard of care for patients with treatment-naive advanced-stage *ROS1* fusion-positive NSCLCs¹³³. Crizotinib has been extensively studied in prospective and retrospective clinical studies (TABLE 1, Supplementary Table 3) and is approved for this indication by multiple regulatory agencies (including those of the USA¹³⁴, Europe¹³⁵, China¹³⁶, Japan, Taiwan¹³⁷, South Korea¹³⁸, Israel¹³⁹ and Australia¹⁴⁰). ORRs with this agent were consistently high, at 65–80%.

In the two largest prospective studies of crizotinib in patients with *ROS1* fusion-positive NSCLCs^{101,141}, the median PFS durations of 16 months and 19 months exceeded the 11-month median PFS duration reported with this agent in patients with treatment-naive advanced-stage *ALK* fusion-positive NSCLCs¹⁴². Thus, crizotinib might provide more durable disease control in patients with *ROS1* fusions versus those with *ALK* fusions. Findings of a retrospective case series have confirmed this observation, and the longer PFS duration in patients with *ROS1* fusion-positive disease was hypothesized to be secondary to the higher potency of crizotinib against ROS1 compared with ALK, rather than due to differences in natural history, given that overall survival was similar in the *ROS1* fusion-positive and *ALK* fusion-positive populations¹⁴³.

The results of one retrospective study indicate that PFS with crizotinib is longer in patients with non-*CD74–ROS1* versus *CD74–ROS1* fusions¹⁴⁴, but this was not the case in a separate series of patients⁵⁴ (Supplementary Table 4). Comparisons in retrospective series indicate that crizotinib is more active than chemotherapy in terms of ORR and PFS in patients with *ROS1*-rearranged NSCLC (Supplementary Table 5). Patients with *ROS1*-rearranged NSCLC treated with crizotinib in PROFILE 1001 (REF.¹⁴¹) had one of the

longest median overall survival durations (4 years and 3 months) achieved in any prospective trial of targeted therapy for metastatic oncogene-driven NSCLCs.

Entrectinib has been studied in three large multicentre trials (ALKA-372-001, STARTRK-1 and STARTRK-2)^{8,145}, the combined results of which led to FDA approval of this drug for the first-line treatment of advanced-stage *ROS1*-rearranged NSCLC. Thus, both crizotinib and entrectinib have received regulatory approval for this indication and consensus guidelines do not specify a preferred agent. However, the regulatory dataset of entrectinib included a high proportion of patients (>40%) with baseline central nervous system (CNS) metastases; the pivotal PROFILE 1001 trial of crizotinib did not include patients with untreated CNS metastases, and only 18% of patients had baseline CNS metastases in the largest trial of crizotinib^{8,101,145}. Despite enrichment for patients with this poor prognostic factor, outcomes with entrectinib remained similar to those with crizotinib (ORR 77% and median PFS 19 months). Bearing in mind the caveats of cross-trial comparisons, entrectinib could potentially be considered over crizotinib for patients with intracranial disease and might delay the development of brain metastasis in patients without intracranial disease.

Other early-generation *ROS1* TKIs, including ceritinib and brigatinib, have documented clinical activity (TABLE 1). Ceritinib is listed in the NCCN guidelines as a first-line treatment option for patients with advanced-stage *ROS1*-rearranged NSCLC¹³³ based on data from a phase II study (ORR 67% and median PFS 19 months)¹⁴⁶, but its use has been limited by the lack of regulatory approval in this setting and substantial gastrointestinal toxicities at the full dose.

Importantly, next-generation TKIs have also been explored in patients with TKI-naive *ROS1*-rearranged NSCLC. These agents include lorlatinib (ORR 62% and median PFS 21 months)¹⁴⁷, repotrectinib (ORR 91%)¹⁴⁸ and taletrectinib (ORR 67%)¹⁴⁹. Of all three TKIs, only repotrectinib has FDA Fast Track Designation (granted in 2020) for the treatment of patients with *ROS1* TKI-naive disease¹⁵⁰. Recognizing that these data are preliminary, the median PFS achieved with lorlatinib is similar to those of early-generation TKIs. This observation implies that, unlike in patients with *EGFR*-mutant¹⁵¹ or *ALK* fusion-positive¹⁴² NSCLCs, next-generation agents have yet to achieve longer durations of disease control than early-generation TKIs. Further data are needed to determine if next-generation TKIs will replace early-generation TKIs as a standard of care in the treatment-naive disease setting.

Other cancers.—*ROS1* TKIs are active in other *ROS1* fusion-positive cancers; however, these drugs have yet to be approved in a histology-agnostic fashion or even for any cancer other than NSCLC. In case series or reports (Supplementary Table 6), activity has been observed against cancers in both children and adults: in atypical meningioma (with a *TFG-ROS1* fusion)¹⁵² or pulmonary blastoma (*CD74-ROS1*)¹⁵³ with crizotinib, and in ER⁺PR⁺HER2⁻ breast cancer (*GOPC-ROS1*)¹⁵⁴ or IMT (*TFG-ROS1*)^{68,155} with ceritinib. The clinical development programme of entrectinib continues to explore the histology-agnostic activity of this drug, with responses observed in patients with IMT (with a *TFG-ROS1* fusion)¹⁵⁶, melanoma (*GOPC-ROS1*)¹²³ or high-grade glioma (*EEFIG-ROS1* or *GOPC-ROS1*)¹⁵⁷. In cohorts of the adult and paediatric NCI-MATCH trials, patients

with *ROS1* fusion-positive cancers are being treated with crizotinib¹⁵⁸ and ensartinib¹⁵⁹, respectively.

Intracranial activity

Activity in the CNS is an important requirement for ROS1 TKIs because *ROS1* fusions are found in both primary brain cancers and brain-metastatic solid tumours. In trials involving patients with advanced-stage NSCLC, the incidence of brain metastases ranges from 20% to 40% in the treatment-naïve setting and from 30% to 50% in patients pre-treated with TKIs^{160,161}. The incidence of leptomeningeal disease has not been reported¹⁶⁰. Earlier reports indicate that brain metastases were less common in patients with *ROS1*-rearranged than in those with *ALK*-rearranged or *RET*-rearranged NSCLCs^{143,161}, although this difference has not been observed in subsequent studies¹⁶². Brain metastases were more frequent in patients with NSCLCs harbouring *CD74-ROS1* than in those with non-*CD74-ROS1* fusions (32% versus 0%; $P = 0.02$) in one series, implying that fusion type might influence the predilection for intracranial metastases¹⁴⁴. Indeed, a preclinical study revealed that *CD74-ROS1* (but not *SLC34A2-ROS1* or *GOPC-ROS1*) activates an invasiveness pathway involving synaptotagmin-1 (*E-Syt1*), which might confer increased metastatic potential to cancer cells⁵⁹.

The CNS activity of early-generation ROS1 TKIs in patients with *ROS1*-rearranged NSCLC is best characterized for entrectinib, with an intracranial ORR of 55%, a median intracranial duration of response of 12.9 months and a median intracranial PFS duration of 7.7 months¹⁶³ (TABLE 1). Preclinically, this drug accumulates at substantial concentrations in the CNS, is active in a mouse model of *NTRK* fusion-positive glioblastoma and results in increased survival relative to that observed with crizotinib in a mouse orthotopic CNS xenograft model of brain-metastatic *ALK* fusion-positive NSCLC¹⁴⁵. By contrast, the intracranial ORR with ceritinib has been reported to be low (29%)¹⁴⁶, and the CNS activity of cabozantinib has only been described in one retrospective report of data from four patients previously treated with crizotinib and ceritinib¹⁶⁴. Cerebrospinal fluid concentrations of crizotinib are typically low, and the intracranial ORR with this agent was 33% in one study¹⁶⁵⁻¹⁶⁷ (TABLE 1). Intracranial progression frequencies in patients treated with crizotinib range from 47% to 83%^{162,167}. Furthermore, the CNS activity of this drug is suboptimal compared with that of next-generation ALK TKIs in *ALK* fusion-positive cancers¹⁶⁸.

Substantial intracranial activity has been demonstrated with the next-generation TKIs lorlatinib (intracranial ORR 64%)¹⁴⁷ and repotrectinib (intracranial ORR 100%)¹⁶⁹ in patients with treatment-naïve *ROS1*-rearranged NSCLC (TABLE 1). With lorlatinib, a complete intracranial response was achieved in a patient with leptomeningeal disease¹⁴⁷. The incidence of CNS progression at 2 years was 29% and 19% in patients who were TKI naïve and in those pre-treated with crizotinib, respectively¹⁴⁷. The intracranial activity of lorlatinib has also been demonstrated in a genetically engineered mouse model of *GOPC-ROS1*-driven glioblastoma¹¹⁸ and a mouse xenograft model of human *GOPC-ROS1*-driven glioblastoma⁵⁰.

ROS1 inhibitor resistance

ROS1-intrinsic mechanisms

Preclinical and clinical studies have identified *ROS1* kinase domain point mutations that result in the resistance of *ROS1* fusion-positive cancers to ROS1 TKIs^{143,170} (FIG. 3a,b). Mutations resulting in substitutions at solvent-front residues (G2032, D2033 and L1951) or the ‘gatekeeper’ residue (L2026) of ROS1 have been identified in tumour specimens from patients (FIG. 3b). Several of these mutations are paralogous to *ALK*, *RET* and/or *NTRK* resistance mutations that emerge with targeted therapy for ALK, RET or TRK fusions¹⁷¹; however, paralogous mutations that result in substitutions involving the xDFG motif of ROS1 (particularly the G2101 residue) have not yet been observed. Furthermore, two or three co-occurring mutations have been identified in the same cancer. Substitutions engendering resistance of *ROS1* fusion-driven cancers to type I TKIs include E1935G, L1947R, L1951R, G1971E, L1982F, S1986F/Y, L2026M, G2032R, D2033N, C2060G, V2098I and L2155S for crizotinib^{60,127–129,143,170,172}, E1990G and F1994L for ceritinib¹²⁹, F2004C/I and G2032R for entrectinib¹⁷³, and S1986F (co-occurred with L2000V in one patient), G2032K/R (G2032R occurred with S1986F and L2086F in one patient) and L2086F for lorlatinib^{174,175}. Although overlap exists, the spectrum of type II TKI resistance can differ from that of type I TKIs (FIG. 4a): substitutions observed with type II ROS1 TKIs include E1974K, F2004V/C, E2020K, V2089M, D2113N/G, M2134I and F2075V/C^{124,176}, none of which involves solvent-front or gatekeeper residues. Notably, concurrent *ROS1* kinase domain mutations (S1986F and S1986Y, and L2026M and L1951R in *trans*) have been reported^{128,170}. This evidence of emergent polyclonal *ROS1* kinase domain mutations indicates that clonal heterogeneity in the resistant-disease setting might pose challenges for second-line, single-agent TKI therapy.

The functional and steric consequences of several *ROS1* mutations are known. ROS1^{G2032R}, the most common resistance substitution observed in patients to date¹⁴³, permits continued ATP binding but leads to steric clash with the piperidine ring of crizotinib and prevents effective binding of this TKI. These findings come from a study that provided the first reported crystal structure of the ROS1 kinase domain in complex with crizotinib (PDB 3ZBF)¹¹³. ROS1^{G2032R} has also been shown to induce epithelial–mesenchymal transition and to increase the migratory and invasive capacities of *ROS1* fusion-driven cancer cells via upregulation of Twist1 (REF.¹⁷⁷). ROS1^{L1951R}, analogous to the ALK^{L1196M} resistance substitution, also creates steric hindrance to crizotinib binding¹²⁹. Similarly, ROS1^{S1986Y/F} hinders crizotinib binding, albeit by inducing a positional change in the α C helix rather than affecting the solvent front¹²⁸. The lorlatinib-resistant ROS1^{L2086F} substitution¹⁷⁵, analogous to the previously described ALK^{L1256F} lorlatinib-resistant substitution, creates steric interference with lorlatinib, crizotinib and entrectinib binding, although sensitivity to cabozantinib might be retained.

ROS1-extrinsic mechanisms

Progression of *ROS1*-rearranged cancers during TKI therapy can occur through ROS1-extrinsic resistance mechanisms (FIG. 3c). Bypass or downstream mediators implicated in this process include KRAS, NRAS, EGFR, HER2, MET, KIT, BRAF and

MEK^{127,128,143,170}. In the clinical setting, *KRAS*^{G12D} and *BRAF*^{V600E} mutations have emerged with crizotinib treatment¹⁷⁸, and *NRAS*^{Q61K} has emerged with entrectinib^{173,179}. Hotspot mutations affecting β -catenin (for example, *CTNNB1*^{S45F}) and activating *PIK3CA* mutations have also been identified post-progression in patients treated with ROS1 TKIs^{105,170}. The spectrum of other kinases inhibited by a particular ROS1 TKI seems to influence the extrinsic resistance mechanisms acquired. For example, *MET* amplification (a resistance mechanism observed in other fusion-positive cancers¹⁸⁰) was not reported as a mediator of ROS1 TKI (lorlatinib) resistance until 2020 (REF.¹⁷⁵). This delay might have been because most of the earliest patients with *ROS1* fusion-positive cancers treated with a ROS1 TKI received crizotinib; therefore, the evolutionary constraints of concurrent *MET* inhibition by this agent might have suppressed the acquisition of *MET*-mediated resistance.

Combination therapy is active preclinically in cancers with ROS1-extrinsic resistance to ROS1 TKIs; however, clinical responses have yet to be reported. First, adaptive EGFR activation was observed in TKI-resistant SLC34A2-ROS1-expressing HCC78 cells¹⁸¹, and co-treatment with gefitinib re-sensitized these cells to ROS1 inhibition¹⁸². Data from another study demonstrated the synergistic activity of crizotinib and afatinib or dacomitinib in crizotinib-resistant HCC78 cells¹⁷². In neither study was an *EGFR* alteration identified in the resistant cells. Clinically, *EGFR* mutations rarely co-occur with *ROS1* fusions de novo^{54,65}; however, *ROS1* fusions do emerge (2% of all acquired fusions) as resistance mechanisms to EGFR TKI therapy in *EGFR*-mutant NSCLCs¹⁸³, implying potential signalling reciprocity or feedback between EGFR and ROS1. Second, increased HER2 phosphorylation has been detected in a patient-derived, crizotinib-resistant *CD74-ROS1*-expressing NSCLC cell line (CUTO23); afatinib co-treatment restored crizotinib sensitivity in this cell line¹⁷⁰. Third, transducing *KIT*^{D816G} into HCC78 or CUTO-2 cells promoted crizotinib resistance¹⁸². Co-treatment with the KIT inhibitor ponatinib re-sensitized these cells to crizotinib¹⁸⁴. Finally, in a series of 75 patients with *ROS1* fusion-positive NSCLCs treated with ROS1 TKIs, eight (11%) were found to have concurrent MAPK alterations, including two patients with *MEK1*delE41_L54 or *MEKK1*delH907_C916 mutations and two with loss-of-function mutations in *NFI* (REF.¹⁸⁵). In subsequent in vitro modelling experiments, *MEK1* or *MEKK1* deletion or *NFI* knockdown conferred resistance to ROS1 TKIs and combined ROS1 and MEK inhibition suppressed the growth of these cells¹⁸⁵.

Heterogeneity of resistance

The contribution of intratumour and intertumour heterogeneity to specific patterns of ROS1 TKI resistance in individual patients remains underexplored. Intertumour heterogeneity has been identified in one report¹⁰⁵ that described a patient with disease progression on crizotinib, in whom a *ROS1*^{G2032R} mutation was identified in plasma cfDNA but not in a biopsy sample obtained from a growing liver lesion. This patient subsequently received combination chemotherapy (carboplatin and pemetrexed) plus crizotinib, resulting in clinical benefit, but with eventual disease progression. On progression, the *ROS1*^{G2032R} mutation was identified in DNA from pleural fluid. In a separate report¹⁴⁷, a patient with disease progression on crizotinib had a *ROS1*^{G2032R} mutation identified in tumour tissue and a *ROS1*^{L2026M} mutation detected in plasma cfDNA. Finally, concurrent high-level *MET* amplification co-occurred with *ROS1*^{G2032R} post lorlatinib resistance in a third report¹⁷⁵.

Collectively, these findings imply that the pressures that drive resistance can result in spatial and/or temporal heterogeneity. Ultimately, genomic heterogeneity can inform therapeutic choices. In particular, when both ROS1-intrinsic and ROS1-extrinsic resistance are detected, reliance solely on next-generation TKIs might not be sufficient. Depending on the nature of the resistance mechanisms in an individual patient, combinations of ROS1-targeted TKIs and/or other standard-of-care therapies (for example, chemotherapy) should be considered.

ROS1 inhibition in TKI-treated cancers

Preclinical activity

Several type I or II inhibitors are active against cancers with *ROS1* fusions harbouring resistance mutations^{60,118–120,124,127–130,186}. The ROS1^{G2032R} solvent-front substitution is largely insensitive to the early-generation inhibitors crizotinib, ceritinib, entrectinib and brigatinib (FIG. 4a). However, repotrectinib and taletrectinib retain inhibitory activity against ROS1^{G2032R}. Specifically, in Ba/F3 CD74–ROS1^{G2032R} cells, the IC₅₀ of repotrectinib is 0.1 nM for the wild-type kinase and 3.3 nM for the ROS1^{G2032R} variant; these values are 0.8 and 13.5 nM, respectively, for taletrectinib. Thus, CD74–ROS1^{G2032R} might remain sensitive to these inhibitors in the clinical setting, given that the modestly increased IC₅₀ values for the mutant protein remain below the achievable plasma concentrations for these agents. By contrast, the potency of lorlatinib against ROS1^{G2032R} is reduced 595-fold: the cell-based IC₅₀ is increased from an average of 0.4 nM for wild-type *ROS1* fusions to an average of 238 nM for ROS1^{G2032R} fusions^{119,120,126–128}.

Lorlatinib is active against cells with ROS1^{S1986F} or ROS1^{S1986Y} substitutions (IC₅₀ 1 nM and 1.6 nM, respectively)¹²⁸ that alter the conformation of the αC-helix, which contains residues that are essential for stabilizing the catalytically active conformation of the kinase domain via interactions with residues in the activation loop and the activation site (FIG. 3b). ROS1^{L1951R} confers resistance to crizotinib, ceritinib and brigatinib, whereas entrectinib, taletrectinib and lorlatinib all have potent activity against cells with this substitution (IC₅₀ <5 nM for all three inhibitors) (FIG. 4a). Repotrectinib has not been tested in ROS1^{L1951R}-containing cells but might be active in this context based on its potency against ROS1^{G2032R}. The lack of activity of early-generation agents against recalcitrant ROS1 kinase domain substitutions explains, in part, the lack of benefit observed in patients following disease progression on prior ROS TKI therapy (TABLE 1).

TKI type switching

The ROS1-intrinsic resistance liabilities imposed by ROS1 TKIs vary by binding mode (type I versus type II) (FIG. 4); therefore, TKI type switching is a compelling concept for mitigating resistance. For example, the ROS1^{D2033N} resistance substitution disrupts the interaction between the negatively charged D2033 residue and the positively charged piperidine ring of crizotinib. By contrast, ROS1 binding by cabozantinib, which achieves optimal type II conformation docking scores in molecular dynamics simulation studies¹²⁴, does not involve interaction with this residue. The type I TKI repotrectinib retains activity against ROS1^{D2033N}, but this alteration decreases the activity of most other type I inhibitors (crizotinib, brigatinib, ceritinib, entrectinib, ensartinib and taletrectinib) and, interestingly,

results in hypersensitization to the type II TKIs cabozantinib and foretinib^{119,127} (FIG. 4a). As a clinical proof of concept, switching to cabozantinib resulted in a confirmed objective response in a patient with NSCLC with ROS1^{D2033N}-mediated resistance to crizotinib¹²⁷. Similarly, the solvent front ROS1^{L2086F} substitution conferred resistance to type I inhibitors lorlatinib, crizotinib and entrectinib but remains at least partially sensitive to the type II inhibitor cabozantinib (with stable disease observed during 10.8 months of treatment in one patient)¹⁷⁵. Conversely, ROS1 fusions with certain type II TKI-resistance mutations remain sensitive to type I TKIs such as crizotinib, ceritinib and brigatinib¹²⁴ (FIG. 4a), underscoring the potential role of type II to type I TKI switching in this context. Moreover, treatment with combinations of type I and II TKIs might increase the durability of disease control by preventing the emergence of subclonal resistant populations.

Clinical activity

The activity of next-generation TKIs against ROS1 fusion-positive cancers has only been explored in patients with NSCLC; ORRs of 33–39% have been demonstrated with these agents in patients with disease progression on a prior TKI (FIG. 5a, Table 1), recognizing that the data are preliminary and have yet to mature. These ORRs imply that ROS1-extrinsic resistance might occur in a substantial proportion of cancers following treatment with an early-generation TKI. This situation would be unlike that in EGFR-mutant or ALK fusion-positive NSCLCs, for which next-generation agents consistently achieve high ORRs (>60%) post-progression on early-generation TKI therapy (for example, with osimertinib post-erlotinib or alectinib post-crizotinib, respectively).

Nevertheless, next-generation TKIs are active in a subgroup of TKI pre-treated patients, and durable responses can be achieved. This highlights the utility of sequential TKI therapy (FIG. 5b). For example, lorlatinib has been associated with an ORR of 35% and a median PFS of 8.5 months in patients pre-treated with crizotinib, although no responses were achieved in patients who received two or more prior TKIs. The intracranial ORR was 50%¹⁴⁷. Responses were observed in patients with cancers harbouring ROS1^{K1991E} or ROS1^{S1986F} but no responses were achieved in those with ROS1^{G2032R} or ROS1^{L2026M}. In one patient with ROS1^{L2026M} detected in both tumour tissue-derived DNA and cfDNA, disease regression was achieved with lorlatinib but disease control only lasted 2.7 months. Considering that lorlatinib has preclinical activity against ROS1^{L2026M}, this finding implicates occult factors such as concurrent ROS1-extrinsic resistance, again highlighting the influence of tumour heterogeneity on the extent of clinical benefit. Lorlatinib is listed in the NCCN guidelines as a treatment option after progression on crizotinib, entrectinib or ceritinib¹³³; however, whether regulatory approval will be pursued in this context remains unclear.

Data on repotrectinib and taletrectinib are less mature and come from small numbers of patients treated at a range of doses (TABLE 1, fig. 5a). In a phase I/II trial, repotrectinib achieved an ORR of 39% at a variety of doses in patients who had received one prior TKI, with an ORR of 57% at the recommended dose in patients pre-treated with crizotinib¹⁸⁷. The overall intracranial ORR was 75% in patients pre-treated with TKIs. Importantly, in contrast to lorlatinib, responses were achieved in patients who received two or more

prior TKIs and in cancers with *ROS1*^{G2032R} (ORR 43%, disease regression occurred in all patients)¹⁶⁹. In a phase I trial¹⁴⁹, taletrectinib resulted in an ORR of 33% in patients pre-treated with crizotinib. *ROS1* mutation status was not determined and, thus, the clinical activity of this agent in the setting of ROS1-intrinsic resistance is currently unknown. In a phase II trial¹²⁷, cabozantinib resulted in an objective response in one patient with *ROS1*-rearranged NSCLC that had progressed after 26 months on crizotinib treatment. Additional patients with post-crizotinib responses to cabozantinib have been reported separately^{126,188}. Of four patients in one retrospective series¹⁶⁴, one had a partial response and three had stable disease, with PFS durations that ranged from 4.9 to 13.8 months.

In summary, given its higher intracranial versus extracranial ORR but its lack of activity against *ROS1*^{G2032R}, lorlatinib can re-establish durable disease control in *ROS1*-rearranged cancers with pharmacokinetic intracranial failure and/or a limited spectrum of resistance mutations. By contrast, repotrectinib is active both intracranially and against a wider spectrum of ROS1-intrinsic resistance mechanisms, including recalcitrant *ROS1* solvent-front substitutions such as *ROS1*^{G2032R}. No next-generation TKI has yet received regulatory approval for the treatment of *ROS1* fusion-positive cancers, although repotrectinib has been granted FDA Fast Track Designation in patients who previously received one ROS1 TKI and platinum-doublet chemotherapy¹⁵⁰.

Consequences of ROS1 inhibition

Effects on native ROS1

The expression of native ROS1 has been examined in preclinical models¹⁸⁹ and in human tissues. In non-human vertebrates (including chickens, rats and mice), *Ros1* expression is spatiotemporally controlled in a cell lineage-specific manner in the kidneys, small intestines, lungs, heart and testis during development, with persistent expression in the lung and testes in adults^{16,18,19}. Interrogation of RNA sequencing data from the Genotype–Tissue Expression (GTEx) Project¹⁹⁰ using the GTEx Portal reveals expression of human *ROS1* in the lung, forebrain, kidney and testis (FIG. 6a). The LungMAP Consortium confirmed *ROS1* expression in non-malignant human lung tissues: single-cell RNA sequencing identified *ROS1* as a signature gene expressed in lung alveolar type II cells¹⁹¹.

ROS1 has an indispensable role in murine testicular maturation. Specifically, transgenic mouse models with ROS1 loss have male-specific infertility without overt anatomical or functional deficits reported in any other organ, under homeostatic conditions^{23,192–200}. In these models, either the loss of expression of ROS1 or its ligand, NELL2, leads to developmental aberrations of epididymal regionalization resulting in infertility; however, acute post-pubertal pharmacological inhibition of ROS1 does not affect fertility in mature male mice²⁰⁰. Evolutionary divergence in organ-specific *ROS1* expression between humans and rodents can be deduced by examining data from a transcriptomic study²⁰¹ in which expression was evaluated in seven organs across developmental time points in eight vertebrate species. In humans, ROS1 is most highly expressed in the lungs and only modestly in the testes. Furthermore, whether NELL2 functions as a ligand for human ROS1 or is the sole ligand in all human organs in which ROS1 is expressed remains unknown. Thus, caution should be exercised when assigning functional roles of human ROS1 based

only on findings in mice. The dearth of knowledge regarding the cellular functions of ROS1 in non-malignant tissues continues to limit our understanding of its physiological role in humans.

Adverse effects in patients

Identifying the clinical consequences of ROS1 inhibition is challenging because a highly selective ROS1 inhibitor has not been developed to date. All prospectively tested ROS1 TKIs potentially inhibit other kinases and, thus, the contribution of ROS1 inhibition to toxicities cannot easily be deconvoluted. In addition, a clear increase in the incidence of any adverse event (AE) has not been seen with more potent, next-generation ROS1 TKIs such as lorlatinib, repotrectinib or taletrectinib. Thus, no singular AE has been definitively associated with ROS1 kinase inhibition in non-neoplastic tissues. Hence, the safety profile of multitarget TKI therapy in patients with *ROS1*-rearranged cancers is largely characterized by AEs of three categories: (1) those observed across TKI classes, (2) those attributable to the concurrent inhibition of kinases other than ROS1 and (3) unique additional AEs associated with particular TKIs (FIG. 6b). AEs of all three categories have been shown to affect dose modification rates (Supplementary Figure 2).

Cross-class AEs of ROS1 TKIs occurring in 10% of patients include fatigue and gastrointestinal toxicities. Importantly, high-grade and sometimes fatal liver toxicities have been observed in patients with NSCLC who received crizotinib sequentially or concurrently with ICIs^{202,203}. Less common AEs (affecting <5% of patients) include pulmonary toxicities, such as pneumonitis and/or interstitial lung disease²⁰⁴, and QTc prolongation.

The second category includes toxicities mediated by TRK and/or MET inhibition. Inhibition of the TRK family of kinases, which have roles in nervous system homeostasis, can result in dizziness and/or ataxia, paresthesias, neuropathy, weight gain and cognitive dysfunction; TRK inhibitor withdrawal can also cause pain flares¹⁷¹. MET inhibition can result in peripheral oedema²⁰⁵.

Finally, unique toxicities are associated with certain TKIs, for which a clear mechanism is poorly described. These toxicities include ophthalmological AEs (for example, photopsia, impaired dark adaptation and/or floaters in the eyes) with crizotinib, brigatinib, entrectinib and lorlatinib^{206,207}, hypercholesterolaemia and/or hypertriglyceridaemia with lorlatinib²⁰⁸, hypertension with brigatinib²⁰⁹ and central adult male hypo gonadism with crizotinib (secondary to hypothalamic–pituitary axis dysfunction and not to the epididymal dysfunction noted with developmental ROS1 loss in mice)²¹⁰.

Conclusions

More than three decades since the discovery of the first *ROS1* fusion, a wealth of knowledge is available on ROS1-targeted therapies for patients with *ROS1* fusion-positive cancers. At least nine TKIs have been investigated²¹¹, two of which have regulatory approval across various countries. Several major resistance mechanisms have been characterized and the activity of next-generation TKIs highlights the possible utility of sequential TKI therapy.

Clinical investigations will be faced with ongoing challenges. For example, conducting randomized phase III trials is difficult given the low frequency of *ROS1* fusion-positive cancers. Furthermore, the utility and ethics of randomizing patients to a control arm with historically lower response rates and shorter survival durations are questionable. Interrogating real-world evidence in multicentre cohorts and global trial registries could help elucidate the activity of standard-of-care therapies in homogeneous cohorts of patients with *ROS1* fusion-positive cancers. This approach could provide ‘synthetic’ control groups sufficient to meet the needs of select regulatory environments.

The future of ROS1 research should now turn towards underexplored questions. Preclinically, the functional role of native ROS1 in non-malignant human cells and tissues remains an enigma and should be studied further, including efforts to validate the role of NELL2, the very recently identified murine ROS1 ligand, in human cells or tissues. The oncogenic potential of *ROS1* mutations and/or amplifications and deregulated or ectopic ROS1 expression requires additional characterization and might unveil opportunities to expand the benefits of ROS1-targeted therapies. Furthermore, the contributions of fusion heterogeneity and subcellular localization to cancer biology remain unknown for most of the fusion subtypes. A deeper understanding of *ROS1* fusion biology might inform future synthetic lethal or other combination targeting strategies.

In the clinic, the activity of chemoimmunotherapy and combinations of TKIs with chemotherapy and/or immunotherapy in patients with *ROS1*-rearranged cancers needs to be determined. Beyond the singular identification of a *ROS1* fusion, assays that capture spatiotemporal genomic heterogeneity might help direct decisions on therapeutic sequencing (FIG. 5b). Lastly, histology-agnostic approval of a ROS1 TKI for any *ROS1* fusion-positive cancer would increase patient access and would therefore be welcomed by many patients and health-care providers.

Supplementary Material

Refer to Web version on PubMed Central for supplementary material.

Acknowledgements

The authors would like to thank Dr Clare Wilhelm for critically reading the manuscript and for editorial contributions. The work of the authors is supported in part by NIH grants (P01 CA129243 and P30 CA008748 to A.D. and R01 CA233495–01A1 to M.A.D.) and an American Cancer Society (ACS) grant (RSG-19–082-01-TBG to M.A.D.).

References

1. Birchmeier C, Sharma S & Wigler M Expression and rearrangement of the ROS1 gene in human glioblastoma cells. *Proc. Natl Acad. Sci. USA* 84, 9270–9274 (1987). [PubMed: 2827175]
2. Sharma S et al. Characterization of the *ros1*-gene products expressed in human glioblastoma cell lines. *Oncogene Res* 5, 91–100 (1989). [PubMed: 2691958]
3. Birchmeier C, O’Neill K, Riggs M & Wigler M Characterization of ROS1 cDNA from a human glioblastoma cell line. *Proc. Natl Acad. Sci. USA* 87, 4799–4803 (1990). [PubMed: 2352949]
4. Charest A et al. Oncogenic targeting of an activated tyrosine kinase to the Golgi apparatus in a glioblastoma. *Proc. Natl Acad. Sci. USA* 100, 916–921 (2003). [PubMed: 12538861]

5. Charest A et al. Fusion of FIG to the receptor tyrosine kinase ROS in a glioblastoma with an interstitial del(6) (q21q21). *Genes Chromosomes Cancer* 37, 58–71 (2003). [PubMed: 12661006]
6. Charest A et al. ROS fusion tyrosine kinase activates a SH2 domain-containing phosphatase-2/ phosphatidylinositol 3-kinase/mammalian target of rapamycin signaling axis to form glioblastoma in mice. *Cancer Res* 66, 7473–7481 (2006). [PubMed: 16885344]
7. Rikova K et al. Global survey of phosphotyrosine signaling identifies oncogenic kinases in lung cancer. *Cell* 131, 1190–1203 (2007). [PubMed: 18083107]
8. Shaw AT et al. Crizotinib in ROS1-rearranged non-small-cell lung cancer. *N. Engl. J. Med* 371, 1963–1971 (2014). [PubMed: 25264305]
9. Chugai Pharmaceutical Co. Ltd. Chugai Obtains Approval for Additional Indication of Rozlytrek for ROS1 Fusion-Positive Non-Small Cell Lung Cancer https://www.roche.com/dam/jcr:6c8d9698-38cf49c7-a25b-5a27acb04ac3/en/200221_IR_Chugai_eRozlytrek_ROS1-NSCLC_Approval.pdf (2020).
10. Feldman RA, Wang LH, Hanafusa H & Balduzzi PC Avian sarcoma virus UR2 encodes a transforming protein which is associated with a unique protein kinase activity. *J. Virol* 42, 228–236 (1982). [PubMed: 6177870]
11. Shibuya M, Hanafusa H & Balduzzi PC Cellular sequences related to three new onc genes of avian sarcoma virus (fps, yes, and ros) and their expression in normal and transformed cells. *J. Virol* 42, 143–152 (1982). [PubMed: 6177868]
12. Neckameyer WS & Wang LH Molecular cloning and characterization of avian sarcoma virus UR2 and comparison of its transforming sequence with those of other avian sarcoma viruses. *J. Virol* 50, 914–921 (1984). [PubMed: 6328022]
13. Neckameyer WS & Wang LH Nucleotide sequence of avian sarcoma virus UR2 and comparison of its transforming gene with other members of the tyrosine protein kinase oncogene family. *J. Virol* 53, 879–884 (1985). [PubMed: 2983097]
14. Notter MF, Navon SE, Fung BK & Balduzzi PC Infection of neuroretinal cells in vitro by avian sarcoma viruses UR1 and UR2: transformation, cell growth stimulation, and changes in transducin levels. *Virology* 160, 489–493 (1987). [PubMed: 2821688]
15. Matsushime H, Wang LH & Shibuya M Human c-ros-1 gene homologous to the v-ros sequence of UR2 sarcoma virus encodes for a transmembrane receptorlike molecule. *Mol. Cell. Biol* 6, 3000–3004 (1986). [PubMed: 3023956]
16. Kanwar YS, Liu ZZ, Kumar A, Wada J & Carone FA Cloning of mouse c-ros renal cDNA, its role in development and relationship to extracellular matrix glycoproteins. *Kidney Int* 48, 1646–1659 (1995). [PubMed: 8544427]
17. Chen J, Tong J, Tanaka-Sukegawa I & Wang LH Cloning and functional characterization of the chicken c-ros promoter. *Cell Growth Differ* 6, 1523–1530 (1995). [PubMed: 9019157]
18. Acquaviva J, Wong R & Charest A The multifaceted roles of the receptor tyrosine kinase ROS in development and cancer. *Biochim. Biophys. Acta* 1795, 37–52 (2009). [PubMed: 18778756]
19. Matsushime H & Shibuya M Tissue-specific expression of rat c-ros-1 gene and partial structural similarity of its predicted products with sev protein of *Drosophila melanogaster*. *J. Virol* 64, 2117–2125 (1990). [PubMed: 2139140]
20. Springer TA An extracellular beta-propeller module predicted in lipoprotein and scavenger receptors, tyrosine kinases, epidermal growth factor precursor, and extracellular matrix components. *J. Mol. Biol* 283, 837–862 (1998). [PubMed: 9790844]
21. Neckameyer WS, Shibuya M, Hsu MT & Wang LH Proto-oncogene c-ros codes for a molecule with structural features common to those of growth factor receptors and displays tissue specific and developmentally regulated expression. *Mol. Cell. Biol* 6, 1478–1486 (1986). [PubMed: 3023892]
22. Shibuya M et al. Analysis of structure and activation of some receptor-type tyrosine kinase oncogenes. *Princess Takamatsu Symp* 17, 195–202 (1986). [PubMed: 3455414]
23. Kiyozumi D et al. NELL2-mediated lumicrine signaling through OVCH2 is required for male fertility. *Science* 368, 1132–1135 (2020). [PubMed: 32499443]

24. Keilhack H et al. Negative regulation of Ros receptor tyrosine kinase signaling. An epithelial function of the SH2 domain protein tyrosine phosphatase SHP-1. *J. Cell Biol* 152, 325–334 (2001). [PubMed: 11266449]
25. Nguyen KT et al. The role of phosphatidylinositol 3-kinase, rho family GTPases, and STAT3 in Ros-induced cell transformation. *J. Biol. Chem* 277, 11107–11115 (2002). [PubMed: 11799110]
26. Riethmacher D, Langholz O, Godecke S, Sachs M & Birchmeier C Biochemical and functional characterization of the murine ros protooncogene. *Oncogene* 9, 3617–3626 (1994). [PubMed: 7970722]
27. Xiong Q, Chan JL, Zong CS & Wang LH Two chimeric receptors of epidermal growth factor receptor and c-Ros that differ in their transmembrane domains have opposite effects on cell growth. *Mol. Cell. Biol* 16, 1509–1518 (1996). [PubMed: 8657124]
28. Zong CS, Zeng L, Jiang Y, Sadowski HB & Wang LH Stat3 plays an important role in oncogenic Ros- and insulin-like growth factor I receptor-induced anchorage-independent growth. *J. Biol. Chem* 273, 28065–28072 (1998). [PubMed: 9774423]
29. Grossmann KS, Rosario M, Birchmeier C & Birchmeier W The tyrosine phosphatase Shp2 in development and cancer. *Adv. Cancer Res* 106, 53–89 (2010). [PubMed: 20399956]
30. Mapstone T, McMichael M & Goldthwait D Expression of platelet-derived growth factors, transforming growth factors, and the ros gene in a variety of primary human brain tumors. *Neurosurgery* 28, 216–222 (1991). [PubMed: 1997889]
31. Watkins D, Dion F, Poisson M, Delattre JY & Rouleau GA Analysis of oncogene expression in primary human gliomas: evidence for increased expression of the ros oncogene. *Cancer Genet. Cytogenet* 72, 130–136 (1994). [PubMed: 8143271]
32. Zhao JF & Sharma S Expression of the ROS1 oncogene for tyrosine receptor kinase in adult human meningiomas. *Cancer Genet. Cytogenet* 83, 148–154 (1995). [PubMed: 7553586]
33. Girish V et al. Bcl2 and ROS1 expression in human meningiomas: an analysis with respect to histological subtype. *Indian J. Pathol. Microbiol* 48, 325–330 (2005). [PubMed: 16761743]
34. Jun HJ et al. Epigenetic regulation of c-ROS receptor tyrosine kinase expression in malignant gliomas. *Cancer Res* 69, 2180–2184 (2009). [PubMed: 19276365]
35. Brennan CW et al. The somatic genomic landscape of glioblastoma. *Cell* 155, 462–477 (2013). [PubMed: 24120142]
36. Cancer Genome Atlas Research Network. Comprehensive genomic characterization defines human glioblastoma genes and core pathways. *Nature* 455, 1061–1068 (2008). [PubMed: 18772890]
37. Shah N et al. Exploration of the gene fusion landscape of glioblastoma using transcriptome sequencing and copy number data. *BMC Genomics* 14, 818 (2013). [PubMed: 24261984]
38. Puchalski RB et al. An anatomic transcriptional atlas of human glioblastoma. *Science* 360, 660–663 (2018). [PubMed: 29748285]
39. Shih CH et al. EZH2-mediated upregulation of ROS1 oncogene promotes oral cancer metastasis. *Oncogene* 36, 6542–6554 (2017). [PubMed: 28759046]
40. Sweet-Cordero A et al. An oncogenic KRAS2 expression signature identified by cross-species gene-expression analysis. *Nat. Genet* 37, 48–55 (2005). [PubMed: 15608639]
41. Sweet-Cordero A et al. Comparison of gene expression and DNA copy number changes in a murine model of lung cancer. *Genes Chromosomes Cancer* 45, 338–348 (2006). [PubMed: 16323170]
42. Bajrami I et al. E-Cadherin/ROS1 inhibitor synthetic lethality in breast cancer. *Cancer Discov* 8, 498–515 (2018). [PubMed: 29610289]
43. US National Library of Medicine. [ClinicalTrials.gov https://clinicaltrials.gov/ct2/show/NCT01939899](https://clinicaltrials.gov/ct2/show/NCT01939899) (2016).
44. Kalla C et al. ROS1 gene rearrangement and expression of splice isoforms in lung cancer, diagnosed by a novel quantitative RT-PCR assay. *J. Mod. Hum. Pathol* 1, 25–34 (2016).
45. Rose-John S & Heinrich PC Soluble receptors for cytokines and growth factors: generation and biological function. *Biochem. J* 300, 281–290 (1994). [PubMed: 8002928]
46. Cerami E et al. The cBio cancer genomics portal: an open platform for exploring multidimensional cancer genomics data. *Cancer Discov* 2, 401–404 (2012). [PubMed: 22588877]

47. Gao J et al. Integrative analysis of complex cancer genomics and clinical profiles using the cBioPortal. *Sci. Signal* 6, pl1 (2013). [PubMed: 23550210]
48. Gu TL et al. Survey of tyrosine kinase signaling reveals ROS kinase fusions in human cholangiocarcinoma. *PLoS ONE* 6, e15640 (2011). [PubMed: 21253578]
49. Lim SM et al. Rare incidence of ROS1 rearrangement in cholangiocarcinoma. *Cancer Res. Treat* 49, 185–192 (2017). [PubMed: 27121721]
50. Davare MA et al. Rare but recurrent ROS1 fusions resulting from chromosome 6q22 microdeletions are targetable oncogenes in glioma. *Clin. Cancer Res* 24, 6471–6482 (2018). [PubMed: 30171048]
51. Rimkunas VM et al. Analysis of receptor tyrosine kinase ROS1-positive tumors in non-small cell lung cancer: identification of a FIG-ROS1 fusion. *Clin. Cancer Res* 18, 4449–4457 (2012). [PubMed: 22661537]
52. Seo JS et al. The transcriptional landscape and mutational profile of lung adenocarcinoma. *Genome Res* 22, 2109–2119 (2012). [PubMed: 22975805]
53. Zhu YC et al. CEP72-ROS1: a novel ROS1 oncogenic fusion variant in lung adenocarcinoma identified by next-generation sequencing. *Thorac. Cancer* 9, 652–655 (2018). [PubMed: 29517860]
54. He Y et al. Different types of ROS1 fusion partners yield comparable efficacy to crizotinib. *Oncol. Res* 27, 901–910 (2019). [PubMed: 30940295]
55. Govindan R et al. Genomic landscape of non-small cell lung cancer in smokers and never-smokers. *Cell* 150, 1121–1134 (2012). [PubMed: 22980976]
56. Park S et al. Characteristics and outcome of ROS1 positive non-small cell lung cancer patients in routine clinical practice. *J. Thorac. Oncol* 13, 1373–1382 (2018). [PubMed: 29883837]
57. Takeuchi K et al. RET, ROS1 and ALK fusions in lung cancer. *Nat. Med* 18, 378–381 (2012). [PubMed: 22327623]
58. Ou SH et al. Identification of a novel TMEM106B-ROS1 fusion variant in lung adenocarcinoma by comprehensive genomic profiling. *Lung Cancer* 88, 352–354 (2015). [PubMed: 25851827]
59. Jun HJ et al. The oncogenic lung cancer fusion kinase CD74-ROS activates a novel invasiveness pathway through E-Syt1 phosphorylation. *Cancer Res* 72, 3764–3774 (2012). [PubMed: 22659450]
60. Davare MA et al. Foretinib is a potent inhibitor of oncogenic ROS1 fusion proteins. *Proc. Natl Acad. Sci. USA* 110, 19519–19524 (2013). [PubMed: 24218589]
61. Saborowski A et al. Mouse model of intrahepatic cholangiocarcinoma validates FIG-ROS as a potent fusion oncogene and therapeutic target. *Proc. Natl Acad. Sci. USA* 110, 19513–19518 (2013). [PubMed: 24154728]
62. Neel DS et al. Differential subcellular localization regulates oncogenic signaling by ROS1 kinase fusion proteins. *Cancer Res* 79, 546–556 (2019). [PubMed: 30538120]
63. Crescenzo R et al. Convergent mutations and kinase fusions lead to oncogenic STAT3 activation in anaplastic large cell lymphoma. *Cancer Cell* 27, 516–532 (2015). [PubMed: 25873174]
64. Arai Y et al. Mouse model for ROS1-rearranged lung cancer. *PLoS ONE* 8, e56010 (2013). [PubMed: 23418494]
65. Wiesweg M et al. High prevalence of concomitant oncogene mutations in prospectively identified patients with ROS1-positive metastatic lung cancer. *J. Thorac. Oncol* 12, 54–64 (2017). [PubMed: 27575422]
66. Lin JJ et al. ROS1 fusions rarely overlap with other oncogenic drivers in non-small cell lung cancer. *J. Thorac. Oncol* 12, 872–877 (2017). [PubMed: 28088512]
67. Antonescu CR et al. Molecular characterization of inflammatory myofibroblastic tumors with frequent ALK and ROS1 gene fusions and rare novel RET rearrangement. *Am. J. Surg. Pathol* 39, 957–967 (2015). [PubMed: 25723109]
68. Lovly CM et al. Inflammatory myofibroblastic tumors harbor multiple potentially actionable kinase fusions. *Cancer Discov* 4, 889–895 (2014). [PubMed: 24875859]
69. Wiesner T et al. Kinase fusions are frequent in Spitz tumours and spitzoid melanomas. *Nat. Commun* 5, 3116 (2014). [PubMed: 24445538]

70. Moeini A, Sia D, Bardeesy N, Mazzaferro V & Llovet JM Molecular pathogenesis and targeted therapies for intrahepatic cholangiocarcinoma. *Clin. Cancer Res* 22, 291–300 (2016). [PubMed: 26405193]
71. Guerreiro Stucklin AS et al. Alterations in ALK/ROS1/NTRK/MET drive a group of infantile hemispheric gliomas. *Nat. Commun* 10, 4343 (2019). [PubMed: 31554817]
72. Bergethon K et al. ROS1 rearrangements define a unique molecular class of lung cancers. *J. Clin. Oncol* 30, 863–870 (2012). [PubMed: 22215748]
73. Parikh DA et al. Characteristics of patients with ROS1⁺ cancers: results from the first patient-designed, global, pan-cancer ROS1 data repository. *JCO Oncol. Pract* 16, e183–e189 (2020). [PubMed: 31880972]
74. Zhu Q, Zhan P, Zhang X, Lv T & Song Y Clinicopathologic characteristics of patients with ROS1 fusion gene in non-small cell lung cancer: a meta-analysis. *Transl. Lung Cancer Res* 4, 300–309 (2015). [PubMed: 26207220]
75. Alexander M et al. A multicenter study of thromboembolic events among patients diagnosed with ROS1-rearranged non-small cell lung cancer. *Lung Cancer* 142, 34–40 (2020). [PubMed: 32087434]
76. Chiari R et al. ROS1-rearranged non-small-cell lung cancer is associated with a high rate of venous thromboembolism: analysis from a phase II, prospective, multicenter, two-arms trial (METROS). *Clin. Lung Cancer* 21, 15–20 (2020). [PubMed: 31607443]
77. Hong DS et al. Phase I study of AMG 337, a highly selective small-molecule MET inhibitor, in patients with advanced solid tumors. *Clin. Cancer Res* 25, 2403–2413 (2019). [PubMed: 30425090]
78. Pan Y et al. ALK, ROS1 and RET fusions in 1139 lung adenocarcinomas: a comprehensive study of common and fusion pattern-specific clinicopathologic, histologic and cytologic features. *Lung Cancer* 84, 121–126 (2014). [PubMed: 24629636]
79. Wahrenbrock M, Borsig L, Le D, Varki N & Varki A Selectin-mucin interactions as a probable molecular explanation for the association of Trousseau syndrome with mucinous adenocarcinomas. *J. Clin. Invest* 112, 853–862 (2003). [PubMed: 12975470]
80. Johnson A et al. Comprehensive genomic profiling of 282 pediatric low- and high-grade gliomas reveals genomic drivers, tumor mutational burden, and hypermutation signatures. *Oncologist* 22, 1478–1490 (2017). [PubMed: 28912153]
81. Richardson TE et al. GOPC-ROS1 fusion due to microdeletion at 6q22 is an oncogenic driver in a subset of pediatric gliomas and glioneuronal tumors. *J. Neuropathol. Exp. Neurol* 78, 1089–1099 (2019). [PubMed: 31626289]
82. Donati M et al. Spitz tumors with ROS1 fusions: a clinicopathological study of 6 cases, including FISH for chromosomal copy number alterations and mutation analysis using next-generation sequencing. *Am. J. Dermatopathol* 42, 92–102 (2020). [PubMed: 31361613]
83. Chen YF et al. Efficacy of pemetrexed-based chemotherapy in patients with ROS1 fusion-positive lung adenocarcinoma compared with in patients harboring other driver mutations in east asian populations. *J. Thorac. Oncol* 11, 1140–1152 (2016). [PubMed: 27094798]
84. Drilon A et al. Clinical outcomes with pemetrexed-based systemic therapies in RET-rearranged lung cancers. *Ann. Oncol* 27, 1286–1291 (2016). [PubMed: 27056998]
85. Kim HR et al. The frequency and impact of ROS1 rearrangement on clinical outcomes in never smokers with lung adenocarcinoma. *Ann. Oncol* 24, 2364–2370 (2013). [PubMed: 23788756]
86. Mazieres J et al. Crizotinib therapy for advanced lung adenocarcinoma and a ROS1 rearrangement: results from the EUROS1 cohort. *J. Clin. Oncol* 33, 992–999 (2015). [PubMed: 25667280]
87. Shen L et al. First-line crizotinib versus platinum-pemetrexed chemotherapy in patients with advanced ROS1-rearranged non-small-cell lung cancer. *Cancer Med* 9, 3310–3318 (2020). [PubMed: 32167664]
88. Song Z, Su H & Zhang Y Patients with ROS1 rearrangement-positive non-small-cell lung cancer benefit from pemetrexed-based chemotherapy. *Cancer Med* 5, 2688–2693 (2016). [PubMed: 27544536]

89. Xu H et al. Crizotinib vs platinum-based chemotherapy as first-line treatment for advanced non-small cell lung cancer with different ROS1 fusion variants. *Cancer Med* 9, 3328–3336 (2020). [PubMed: 32168429]
90. Zhang L et al. Efficacy of crizotinib and pemetrexed-based chemotherapy in Chinese NSCLC patients with ROS1 rearrangement. *Oncotarget* 7, 75145–75154 (2016). [PubMed: 27738334]
91. Rangachari D et al. Correlation between classic driver oncogene mutations in EGFR, ALK, or ROS1 and 22C3-PD-L1 50% expression in lung adenocarcinoma. *J. Thorac. Oncol* 12, 878–883 (2017). [PubMed: 28104537]
92. Jiang L et al. PD-L1 expression and its relationship with oncogenic drivers in non-small cell lung cancer (NSCLC). *Oncotarget* 8, 26845–26857 (2017). [PubMed: 28460468]
93. Mazieres J et al. Immune checkpoint inhibitors for patients with advanced lung cancer and oncogenic driver alterations: results from the IMMUNOTARGET registry. *Ann. Oncol* 30, 1321–1328 (2019). [PubMed: 31125062]
94. Benayed R et al. High yield of RNA sequencing for targetable kinase fusions in lung adenocarcinomas with no mitogenic driver alteration detected by DNA sequencing and low tumor mutation burden. *Clin. Cancer Res* 25, 4712–4722 (2019). [PubMed: 31028088]
95. Schram AM, Chang MT, Jonsson P & Drilon A Fusions in solid tumours: diagnostic strategies, targeted therapy, and acquired resistance. *Nat. Rev. Clin. Oncol* 14, 735–748 (2017). [PubMed: 28857077]
96. Rossi G et al. Detection of ROS1 rearrangement in non-small cell lung cancer: current and future perspectives. *Lung Cancer* 8, 45–55 (2017). [PubMed: 28740441]
97. Cao B et al. Detection of lung adenocarcinoma with ROS1 rearrangement by IHC, FISH, and RT-PCR and analysis of its clinicopathologic features. *Onco Targets Ther* 9, 131–138 (2016). [PubMed: 26770062]
98. Heydt C et al. Comparison of in Situ and extraction-based methods for the detection of ROS1 rearrangements in solid tumors. *J. Mol. Diagn* 21, 971–984 (2019). [PubMed: 31382035]
99. Davies KD et al. Comparison of molecular testing modalities for detection of ROS1 rearrangements in a cohort of positive patient samples. *J. Thorac. Oncol* 13, 1474–1482 (2018). [PubMed: 29935306]
100. Davies KD et al. Identifying and targeting ROS1 gene fusions in non-small cell lung cancer. *Clin. Cancer Res* 18, 4570–4579 (2012). [PubMed: 22919003]
101. Wu YL et al. Phase II study of crizotinib in East Asian patients with ROS1-positive advanced non-small-cell lung cancer. *J. Clin. Oncol* 36, 1405–1411 (2018). [PubMed: 29596029]
102. AmoyDx. AmoyDx ROS1 kit approval in Taiwan, China <http://www.amoydiagnostics.com/newDetail/44> (2018).
103. Drilon A et al. Broad, hybrid capture-based next-generation sequencing identifies actionable genomic alterations in lung adenocarcinomas otherwise negative for such alterations by other genomic testing approaches. *Clin. Cancer Res* 21, 3631–3639 (2015). [PubMed: 25567908]
104. Jordan EJ et al. Prospective comprehensive molecular characterization of lung adenocarcinomas for efficient patient matching to approved and emerging therapies. *Cancer Discov* 7, 596–609 (2017). [PubMed: 28336552]
105. Dagogo-Jack I et al. Molecular analysis of plasma from patients with ROS1-positive NSCLC. *J. Thorac. Oncol* 14, 816–824 (2019). [PubMed: 30664990]
106. PR Newswire. ArcherDX's companion diagnostic assay for both liquid biopsy and tissue specimens granted breakthrough device designation by U.S. Food and Drug Administration <https://www.prnewswire.com/news-releases/archerdxs-companion-diagnostic-assay-for-both-liquid-biopsy-and-tissue-specimens-granted-breakthrough-device-designation-by-us-food-and-drug-administration-300774247.html> (2019).
107. US Food and Drug Administration. Premarket approval of the Oncomine Dx Target Test https://www.accessdata.fda.gov/cdrh_docs/pdf16/P160045A.pdf (2017).
108. Pavlakis N et al. Australian consensus statement for best practice ROS1 testing in advanced non-small cell lung cancer. *Pathology* 51, 673–680 (2019). [PubMed: 31668406]
109. Sholl LM et al. ROS1 immunohistochemistry for detection of ROS1-rearranged lung adenocarcinomas. *Am. J. Surg. Pathol* 37, 1441–1449 (2013). [PubMed: 23887156]

110. Hofman V et al. Multicenter evaluation of a novel ROS1 immunohistochemistry assay (SP384) for detection of ROS1 rearrangements in a large cohort of lung adenocarcinoma patients. *J. Thorac. Oncol* 14, 1204–1212 (2019). [PubMed: 30999109]
111. Conde E et al. Assessment of a new ROS1 immunohistochemistry clone (SP384) for the identification of ROS1 rearrangements in patients with non-small cell lung carcinoma: the ROSING study. *J. Thorac. Oncol* 14, 2120–2132 (2019). [PubMed: 31349061]
112. Huang RSP et al. Correlation of ROS1 immunohistochemistry with ROS1 fusion status determined by fluorescence in situ hybridization. *Arch. Pathol. Lab. Med* 144, 735–741 (2020). [PubMed: 31509456]
113. Awad MM et al. Acquired resistance to crizotinib from a mutation in CD74-ROS1. *N. Engl. J. Med* 368, 2395–2401 (2013). [PubMed: 23724914]
114. Menichincheri M et al. Discovery of entrectinib: a new 3-aminoindazole as a potent anaplastic lymphoma kinase (ALK), c-ros oncogene 1 kinase (ROS1), and pan-tropomyosin receptor kinases (pan-TRKs) inhibitor. *J. Med. Chem* 59, 3392–3408 (2016). [PubMed: 27003761]
115. Marsilje TH et al. Synthesis, structure-activity relationships, and in vivo efficacy of the novel potent and selective anaplastic lymphoma kinase (ALK) inhibitor 5-chloro-N2-(2-isopropoxy-5-methyl-4(piperidin-4-yl)phenyl)-N4-(2-(isopropylsulfanyl)phenyl)pyrimidine-2,4-diamine (LDK378) currently in phase 1 and phase 2 clinical trials. *J. Med. Chem* 56, 5675–5690 (2013). [PubMed: 23742252]
116. Zhang S et al. The potent ALK inhibitor brigatinib (AP26113) overcomes mechanisms of resistance to first- and second-generation ALK inhibitors in preclinical models. *Clin. Cancer Res* 22, 5527–5538 (2016). [PubMed: 27780853]
117. Lovly CM et al. Insights into ALK-driven cancers revealed through development of novel ALK tyrosine kinase inhibitors. *Cancer Res* 71, 4920–4931 (2011). [PubMed: 21613408]
118. Zou HY et al. PF-06463922 is a potent and selective next-generation ROS1/ALK inhibitor capable of blocking crizotinib-resistant ROS1 mutations. *Proc. Natl Acad. Sci. USA* 112, 3493–3498 (2015). [PubMed: 25733882]
119. Drilon A et al. Repotrectinib (TPX-0005) is a next-generation ROS1/TRK/ALK inhibitor that potently inhibits ROS1/TRK/ALK solvent-front mutations. *Cancer Discov* 8, 1227–1236 (2018). [PubMed: 30093503]
120. Katayama R et al. The new-generation selective ROS1/NTRK inhibitor DS-6051b overcomes crizotinib resistant ROS1-G2032R mutation in preclinical models. *Nat. Commun* 10, 3604 (2019). [PubMed: 31399568]
121. Treiber DK & Shah NP Ins and outs of kinase DFG motifs. *Chem. Biol* 20, 745–746 (2013). [PubMed: 23790484]
122. Hubbard SR & Till JH Protein tyrosine kinase structure and function. *Annu. Rev. Biochem* 69, 373–398 (2000). [PubMed: 10966463]
123. Drilon A et al. Safety and antitumor activity of the multitargeted pan-TRK, ROS1, and ALK inhibitor entrectinib: combined results from two phase I trials (ALKA-372-001 and STARTRK-1). *Cancer Discov* 7, 400–409 (2017). [PubMed: 28183697]
124. Davare MA et al. Structural insight into selectivity and resistance profiles of ROS1 tyrosine kinase inhibitors. *Proc. Natl Acad. Sci. USA* 112, E5381–E5390 (2015). [PubMed: 26372962]
125. Yasuda H, de Figueiredo-Pontes LL, Kobayashi S & Costa DB Preclinical rationale for use of the clinically available multitargeted tyrosine kinase inhibitor crizotinib in ROS1-translocated lung cancer. *J. Thorac. Oncol* 7, 1086–1090 (2012). [PubMed: 22617245]
126. Chong CR et al. Identification of existing drugs that effectively target NTRK1 and ROS1 rearrangements in lung cancer. *Clin. Cancer Res* 23, 204–213 (2017). [PubMed: 27370605]
127. Drilon A et al. A novel crizotinib-resistant solvent-front mutation responsive to cabozantinib therapy in a patient with ROS1-rearranged lung cancer. *Clin. Cancer Res* 22, 2351–2358 (2016). [PubMed: 26673800]
128. Facchinetti F et al. Crizotinib-resistant ROS1 mutations reveal a predictive kinase inhibitor sensitivity model for ROS1- and ALK-rearranged lung cancers. *Clin. Cancer Res* 22, 5983–5991 (2016). [PubMed: 27401242]

129. Zou HY et al. PF-06463922, an ALK/ROS1 inhibitor, overcomes resistance to first and second generation ALK inhibitors in preclinical models. *Cancer Cell* 28, 70–81 (2015). [PubMed: 26144315]
130. Ogura H et al. TKI-addicted ROS1-rearranged cells are destined to survival or death by the intensity of ROS1 kinase activity. *Sci. Rep* 7, 5519 (2017). [PubMed: 28717217]
131. Inoue M et al. Mouse models for ROS1-fusion-positive lung cancers and their application to the analysis of multikinase inhibitor efficiency. *Carcinogenesis* 37, 452–460 (2016). [PubMed: 26964870]
132. Ardini E et al. Entrectinib, a pan-TRK, ROS1, and ALK inhibitor with activity in multiple molecularly defined cancer indications. *Mol. Cancer Ther* 15, 628–639 (2016). [PubMed: 26939704]
133. National Comprehensive Cancer Network. NCCN Clinical Practice Guidelines in Oncology (NCCN Guidelines): Non-Small Cell Lung Cancer https://www.nccn.org/professionals/physician_gls/pdf/nscl.pdf (2020).
134. US Food and Drug Administration. FDA approves crizotinib capsules <https://www.fda.gov/drugs/resources-information-approved-drugs/fda-approves-crizotinib-capsules> (2016).
135. Committee for Medicinal Products for Human Use (CHMP). Assessment report: Xalkori https://www.ema.europa.eu/en/documents/variation-report/xalkori-h-c2489-ii-0039-epar-assessment-report-variation_en.pdf (2016).
136. Liu C et al. Crizotinib in Chinese patients with ROS1-rearranged advanced nonsmall-cell lung cancer in routine clinical practice. *Target. Oncol* 14, 315–323 (2019). [PubMed: 30976989]
137. OxOnc Services Company. OxOnc announces that co-development partner has received approval in Japan and Taiwan for crizotinib (Xalkori®) as a first-line treatment for patients with ROS1-positive non-small cell lung cancer <https://www.globenewswire.com/news-release/2017/06/02/1006285/0/en/OxOnc-Announces-that-Co-development-Partner-Has-Received-Approval-in-Japan-and-Taiwan-for-Crizotinib-Xalkori-as-a-First-line-Treatment-for-Patients-with-ROS1-Positive-Non-Small-Cel.html> (2017).
138. Choi W-S Pfizer crizotinib enters ROS1-positive target market [In Korean] <https://www.doctorsnews.co.kr/news/articleView.html?idxno=128964> (2019).
139. State of Israel Ministry of Health. Xalkori – full prescribing information https://www.health.gov.il/units/pharmacy/trufot/alonim/Xalkori_DR_1444888564767.pdf (2015).
140. Australian Government Department of Health. Australian Public Assessment Report for Crizotinib <https://www.tga.gov.au/sites/default/files/auspar-crizotinib-181018.pdf> (2017).
141. Shaw AT et al. Crizotinib in ROS1-rearranged advanced non-small-cell lung cancer (NSCLC): updated results, including overall survival, from PROFILE 1001. *Ann. Oncol* 30, 1121–1126 (2019). [PubMed: 30980071]
142. Peters S et al. Alectinib versus crizotinib in untreated ALK-positive non-small-cell lung cancer. *N. Engl. J. Med* 377, 829–838 (2017). [PubMed: 28586279]
143. Gainor JF et al. Patterns of metastatic spread and mechanisms of resistance to crizotinib in ROS1-positive non-small-cell lung cancer. *JCO Precis. Oncol* 10.1200/PO.17.00063 (2017).
144. Li Z et al. Efficacy of crizotinib among different types of ROS1 fusion partners in patients with ROS1-rearranged non-small cell lung cancer. *J. Thorac. Oncol* 13, 987–995 (2018). [PubMed: 29704675]
145. Drilon A et al. Entrectinib in ROS1 fusion-positive non-small-cell lung cancer: integrated analysis of three phase 1–2 trials. *Lancet Oncol* 21, 261–270 (2020). [PubMed: 31838015]
146. Lim SM et al. Open-label, multicenter, phase II study of ceritinib in patients with non-small-cell lung cancer harboring ROS1 rearrangement. *J. Clin. Oncol* 35, 2613–2618 (2017). [PubMed: 28520527]
147. Shaw AT et al. Lorlatinib in advanced ROS1-positive non-small-cell lung cancer: a multicentre, open-label, single-arm, phase 1–2 trial. *Lancet Oncol* 20, 1691–1701 (2019). [PubMed: 31669155]
148. Drilon A et al. Abstract 442: Repotrectinib, a next generation TRK inhibitor, overcomes TRK resistance mutations including solvent front, gatekeeper and compound mutations. *Cancer Res* 79, 442–442 (2019).

149. Fujiwara Y et al. Safety and pharmacokinetics of DS-6051b in Japanese patients with non-small cell lung cancer harboring ROS1 fusions: a phase I study. *Oncotarget* 9, 23729–23737 (2018). [PubMed: 29805770]
150. Turning Point Therapeutics. Turning Point Therapeutics Reports First-Quarter Financial Results, Provides Update on Operations and COVID-19 Response <https://ir.tptherapeutics.com/node/7186/pdf> (2020).
151. Ramalingam SS et al. Overall survival with osimertinib in untreated, EGFR-mutated advanced NSCLC. *N. Engl. J. Med* 382, 41–50 (2020). [PubMed: 31751012]
152. Rossing M et al. Genomic diagnostics leading to the identification of a TFG-ROS1 fusion in a child with possible atypical meningioma. *Cancer Genet* 212–213, 32–37 (2017).
153. Meng Z et al. A patient with classic biphasic pulmonary blastoma harboring CD74-ROS1 fusion responds to crizotinib. *Onco Targets Ther* 11, 157–161 (2018). [PubMed: 29343973]
154. Parsons BM et al. Abstract 1317: exceptional responses to crizotinib in breast cancer patients with somatic MET and ROS1 alterations. *Cancer Res* 79, 1317–1317 (2019).
155. Li Y et al. Partial response to ceritinib in a patient with abdominal inflammatory myofibroblastic tumor carrying a TFG-ROS1 fusion. *J. Natl Compr. Canc Netw* 17, 1459–1462 (2019). [PubMed: 31805529]
156. Ambati SR, Slotkin EK, Chow-Maneval E & Basu EM Entrectinib in two pediatric patients with inflammatory myofibroblastic tumors harboring ROS1 or ALK gene fusions. *JCO Precis. Oncol* 10.1200/PO.18.00095 (2018).
157. Robinson GW et al. Phase I/IB trial to assess the activity of entrectinib in children and adolescents with recurrent or refractory solid tumors including central nervous system (CNS) tumors. *J. Clin. Oncol* 37 (Suppl. 15), 10009 (2019).
158. US National Library of Medicine. *ClinicalTrials.gov* <https://clinicaltrials.gov/ct2/show/NCT02465060> (2020).
159. US National Library of Medicine. *ClinicalTrials.gov* <https://clinicaltrials.gov/ct2/show/NCT03213652> (2020).
160. Ou SI & Zhu VW CNS metastasis in ROS1⁺ NSCLC: an urgent call to action, to understand, and to overcome. *Lung Cancer* 130, 201–207 (2019). [PubMed: 30885345]
161. Drilon A et al. Frequency of brain metastases and multikinase inhibitor outcomes in patients with RET-rearranged lung cancers. *J. Thorac. Oncol* 13, 1595–1601 (2018). [PubMed: 30017832]
162. Patil T et al. The incidence of brain metastases in stage IV ROS1-rearranged non-small cell lung cancer and rate of central nervous system progression on crizotinib. *J. Thorac. Oncol* 13, 1717–1726 (2018). [PubMed: 29981925]
163. Drilon A et al. Abstract CT192: Entrectinib in locally advanced or metastatic ROS1 fusion-positive non-small cell lung cancer (NSCLC): integrated analysis of ALKA-372-001, STARTRK-1 and STARTRK-2. *Cancer Res* 79, CT192 (2019).
164. Sun TY, Niu X, Chakraborty A, Neal JW & Wakelee HA Lengthy progression-free survival and intracranial activity of cabozantinib in patients with crizotinib and ceritinib-resistant ROS1-positive non-small cell lung cancer. *J. Thorac. Oncol* 14, e21–e24 (2019). [PubMed: 30217491]
165. Costa DB et al. CSF concentration of the anaplastic lymphoma kinase inhibitor crizotinib. *J. Clin. Oncol* 29, e443–e445 (2011). [PubMed: 21422405]
166. Okimoto T et al. A low crizotinib concentration in the cerebrospinal fluid causes ineffective treatment of anaplastic lymphoma kinase-positive non-small cell lung cancer with carcinomatous meningitis. *Intern. Med* 58, 703–705 (2019). [PubMed: 30333394]
167. Landi L et al. Crizotinib in MET-deregulated or ROS1-rearranged pretreated non-small cell lung cancer (METROS): a phase II, prospective, multicenter, two-arms trial. *Clin. Cancer Res* 25, 7312–7319 (2019). [PubMed: 31416808]
168. Gadgeel S et al. Alectinib versus crizotinib in treatment-naïve anaplastic lymphoma kinase-positive (ALK⁺) non-small-cell lung cancer: CNS efficacy results from the ALEX study. *Ann. Oncol* 29, 2214–2222 (2018). [PubMed: 30215676]
169. Cho BC et al. Safety and preliminary clinical activity of repotrectinib in patients with advanced ROS1 fusion-positive non-small cell lung cancer (TRIDENT-1 study). *J. Clin. Oncol* 37, 9011 (2019).

170. McCoach CE et al. Resistance mechanisms to targeted therapies in ROS1⁺ and ALK⁺ non-small cell lung cancer. *Clin. Cancer Res* 24, 3334–3347 (2018). [PubMed: 29636358]
171. Cocco E, Scaltriti M & Drilon A NTRK fusion-positive cancers and TRK inhibitor therapy. *Nat. Rev. Clin. Oncol* 15, 731–747 (2018). [PubMed: 30333516]
172. Song A et al. Molecular changes associated with acquired resistance to crizotinib in ROS1-rearranged non-small cell lung cancer. *Clin. Cancer Res* 21, 2379–2387 (2015). [PubMed: 25688157]
173. Doebele RC et al. Genomic landscape of entrectinib resistance from ctDNA analysis in STARTRK-2. *Ann. Oncol* 30, v865 (2019).
174. Zhou Y et al. A novel ROS1 G2032 K missense mutation mediates lorlatinib resistance in a patient with ROS1-rearranged lung adenocarcinoma but responds to nab-paclitaxel plus pembrolizumab. *Lung Cancer* 143, 55–59 (2020). [PubMed: 32208297]
175. Lin JJ et al. Resistance to lorlatinib in ROS1 fusion-positive non-small cell lung cancer. *J. Clin. Oncol* 38, 9611–9611 (2020).
176. Ogura H et al. TKI-addicted ROS1-rearranged cells are destined to survival or death by the intensity of ROS1 kinase activity. *Sci. Rep* 7, 5519 (2017). [PubMed: 28717217]
177. Gou W et al. CD74-ROS1 G2032R mutation transcriptionally up-regulates Twist1 in non-small cell lung cancer cells leading to increased migration, invasion, and resistance to crizotinib. *Cancer Lett* 422, 19–28 (2018). [PubMed: 29477381]
178. Watanabe J, Furuya N & Fujiwara Y Appearance of a BRAF mutation conferring resistance to crizotinib in non-small cell lung cancer harboring oncogenic ROS1 fusion. *J. Thorac. Oncol* 13, e66–e69 (2018). [PubMed: 29576302]
179. Zhu YC et al. Concurrent ROS1 gene rearrangement and KRAS mutation in lung adenocarcinoma: a case report and literature review. *Thorac. Cancer* 9, 159–163 (2018). [PubMed: 28971587]
180. Cocco E et al. Resistance to TRK inhibition mediated by convergent MAPK pathway activation. *Nat. Med* 25, 1422–1427 (2019). [PubMed: 31406350]
181. Vaishnavi A et al. EGFR mediates responses to small-molecule drugs targeting oncogenic fusion kinases. *Cancer Res* 77, 3551–3563 (2017). [PubMed: 28428274]
182. Davies KD et al. Resistance to ROS1 inhibition mediated by EGFR pathway activation in non-small cell lung cancer. *PLoS ONE* 8, e82236 (2013). [PubMed: 24349229]
183. Zhu VW, Klempner SJ & Ou SI Receptor tyrosine kinase fusions as an actionable resistance mechanism to EGFR TKIs in EGFR-mutant non-small-cell lung cancer. *Trends Cancer* 5, 677–692 (2019). [PubMed: 31735287]
184. Dziadziuszko R et al. An activating KIT mutation induces crizotinib resistance in ROS1-positive lung cancer. *J. Thorac. Oncol* 11, 1273–1281 (2016). [PubMed: 27068398]
185. Sato H et al. MAPK pathway alterations correlate with poor survival and drive resistance to therapy in patients with lung cancers driven by ROS1 fusions. *Clin. Cancer Res* 26, 2932–2945 (2020). [PubMed: 32122926]
186. Song A et al. Molecular changes associated with acquired resistance to crizotinib in ROS1-rearranged non-small cell lung cancer. *Clin. Cancer Res* 21, 2379–2387 (2015). [PubMed: 25688157]
187. Drilon A et al. 444PD - Safety and preliminary clinical activity of repotrectinib in patients with advanced ROS1/TRK fusion-positive solid tumors (TRIDENT-1 study). *Ann. Oncol* 30 (Suppl. 5), 162 (2019).
188. Sun TY, Niu X, Chakraborty A, Neal JW & Wakelee HA Lengthy progression-free survival and intracranial activity of cabozantinib in patients with crizotinib and ceritinib-resistant ROS1-positive non-small cell lung cancer. *J. Thorac. Oncol* 14, e21–e24 (2019). [PubMed: 30217491]
189. Chen J, Zong CS & Wang LH Tissue and epithelial cell-specific expression of chicken proto-oncogene c-ros in several organs suggests that it may play roles in their development and mature functions. *Oncogene* 9, 773–780 (1994). [PubMed: 8108119]
190. GTEx Consortium. The genotype-tissue expression (GTEx) project. *Nat. Genet* 45, 580–585 (2013). [PubMed: 23715323]

191. LungMAP. ROS1 <https://lungmap.net/breath-searchpage/?searchCategory=gene&query=ROS1> (2020). The results referred to here are in whole or part based upon data generated by the LungMAP Consortium [U01HL122642] and downloaded from (www.lungmap.net), on June 23, 2016. The LungMAP consortium and the LungMAP Data Coordinating Center (1U01HL122638) are funded by the National Heart, Lung, and Blood Institute (NHLBI).
192. Cooper TG et al. Gene and protein expression in the epididymis of infertile c-ros receptor tyrosine kinase-deficient mice. *Biol. Reprod* 69, 1750–1762 (2003). [PubMed: 12890734]
193. Cooper TG et al. Mouse models of infertility due to swollen spermatozoa. *Mol. Cell. Endocrinol* 216, 55–63 (2004). [PubMed: 15109745]
194. Sonnenberg-Riethmacher E, Walter B, Riethmacher D, Godecke S & Birchmeier C The c-ros tyrosine kinase receptor controls regionalization and differentiation of epithelial cells in the epididymis. *Genes Dev* 10, 1184–1193 (1996). [PubMed: 8675006]
195. Wagenfeld A, Yeung CH, Lehnert W, Nieschlag E & Cooper TG Lack of glutamate transporter EAAC1 in the epididymis of infertile c-ros receptor tyrosine-kinase deficient mice. *J. Androl* 23, 772–782 (2002). [PubMed: 12399522]
196. Yeung CH, Anapolski M, Setiawan I, Lang F & Cooper TG Effects of putative epididymal osmolytes on sperm volume regulation of fertile and infertile c-ros transgenic Mice. *J. Androl* 25, 216–223 (2004). [PubMed: 14760007]
197. Yeung CH, Sonnenberg-Riethmacher E & Cooper TG Receptor tyrosine kinase c-ros knockout mice as a model for the study of epididymal regulation of sperm function. *J. Reprod. Fertil. Suppl* 53, 137–147 (1998). [PubMed: 10645273]
198. Yeung CH, Sonnenberg-Riethmacher E & Cooper TG Infertile spermatozoa of c-ros tyrosine kinase receptor knockout mice show flagellar angulation and maturational defects in cell volume regulatory mechanisms. *Biol. Reprod* 61, 1062–1069 (1999). [PubMed: 10491645]
199. Yeung CH, Wagenfeld A, Nieschlag E & Cooper TG The cause of infertility of male c-ros tyrosine kinase receptor knockout mice. *Biol. Reprod* 63, 612–618 (2000). [PubMed: 10906072]
200. Jun HJ et al. ROS1 signaling regulates epithelial differentiation in the epididymis. *Endocrinology* 155, 3661–3673 (2014). [PubMed: 24971615]
201. Cardoso-Moreira M et al. Gene expression across mammalian organ development. *Nature* 571, 505–509 (2019). [PubMed: 31243369]
202. Spigel DR et al. Phase 1/2 study of the safety and tolerability of nivolumab plus crizotinib for the first-line treatment of anaplastic lymphoma kinase translocation - positive advanced non-small cell lung cancer (CheckMate 370). *J. Thorac. Oncol* 13, 682–688 (2018). [PubMed: 29518553]
203. Lin JJ et al. Increased hepatotoxicity associated with sequential immune checkpoint inhibitor and crizotinib therapy in patients with non-small cell lung cancer. *J. Thorac. Oncol* 14, 135–140 (2019). [PubMed: 30205166]
204. Pellegrino B et al. Lung toxicity in non-small-cell lung cancer patients exposed to alk inhibitors: report of a peculiar case and systematic review of the literature. *Clin. Lung Cancer* 19, e151–e161 (2018). [PubMed: 29174221]
205. Drilon A et al. Antitumor activity of crizotinib in lung cancers harboring a MET exon 14 alteration. *Nat. Med* 26, 47–51 (2020). [PubMed: 31932802]
206. Ishii T et al. Crizotinib-induced abnormal signal processing in the retina. *PLoS ONE* 10, e0135521 (2015). [PubMed: 26271036]
207. Liu CN et al. Crizotinib reduces the rate of dark adaptation in the rat retina independent of ALK inhibition. *Toxicol. Sci* 143, 116–125 (2015). [PubMed: 25326243]
208. Bauer TM et al. Clinical management of adverse events associated with lorlatinib. *Oncologist* 24, 1103–1110 (2019). [PubMed: 30890623]
209. Stirrups R Brigatinib versus crizotinib for ALK-positive NSCLC. *Lancet Oncol* 19, e585 (2018). [PubMed: 30293790]
210. Weickhardt AJ et al. Rapid-onset hypogonadism secondary to crizotinib use in men with metastatic nonsmall cell lung cancer. *Cancer* 118, 5302–5309 (2012). [PubMed: 22488744]
211. Liu D et al. Characterization of on-target adverse events caused by TRK inhibitor therapy. *Ann. Oncol* 10.1016/j.annonc.2020.05.006 (2020).

212. Michels S et al. Safety and efficacy of crizotinib in patients with advanced or metastatic ROS1-rearranged lung cancer (EUCROSS): a European phase II clinical trial. *J. Thorac. Oncol* 14, 1266–1276 (2019). [PubMed: 30978502]
213. Moro-Sibilot D et al. Crizotinib in c-MET- or ROS1-positive NSCLC: results of the AcSe phase II trial. *Ann. Oncol* 30, 1985–1991 (2019). [PubMed: 31584608]
214. Gettinger SN et al. Activity and safety of brigatinib in ALK-rearranged non-small-cell lung cancer and other malignancies: a single-arm, open-label, phase 1/2 trial. *Lancet Oncol* 17, 1683–1696 (2016). [PubMed: 27836716]
215. Zeng L et al. Vav3 mediates receptor protein tyrosine kinase signaling, regulates GTPase activity, modulates cell morphology, and induces cell transformation. *Mol. Cell. Biol* 20, 9212–9224 (2000). [PubMed: 11094073]
216. GTEx Consortium. The genotype-tissue expression (GTEx) project. *Nat. Genet* 45, 580–585 (2013). [PubMed: 23715323]

Key points

- The proto-oncogene *ROS1* encodes the receptor tyrosine kinase roS1 with an unclear physiological role in humans.
- Chromosomal rearrangement resulting in *ROS1* fusion is the main mechanism underlying roS1-driven oncogenesis. most *ROS1* mutations have unknown significance, and deregulated roS1 expression is probably, at most, a secondary oncogenic mediator.
- *ROS1* fusions can be challenging to detect. Whereas no diagnostic assay is without limitations, the use of complementary Dna-based and rna-based sequencing assays can maximize the identification of *ROS1* fusions; immunohistochemistry is a proposed screening assay.
- Cancers with diverse cellular origins can be driven by *ROS1* fusions in both adults and children; however, roS1 inhibitors are only approved for *ROS1* fusion-positive non-small-cell lung cancers and have yet to receive a histology-agnostic indication.
- The spectrum of roS1-dependent and/or roS1-independent resistance can be influenced by the subcellular localization of the fusion protein, the mode of drug binding (type I versus type II) and the profile of non-roS1-kinase inhibition. The contribution of polyclonality to roS1 inhibitor resistance remains underexplored.

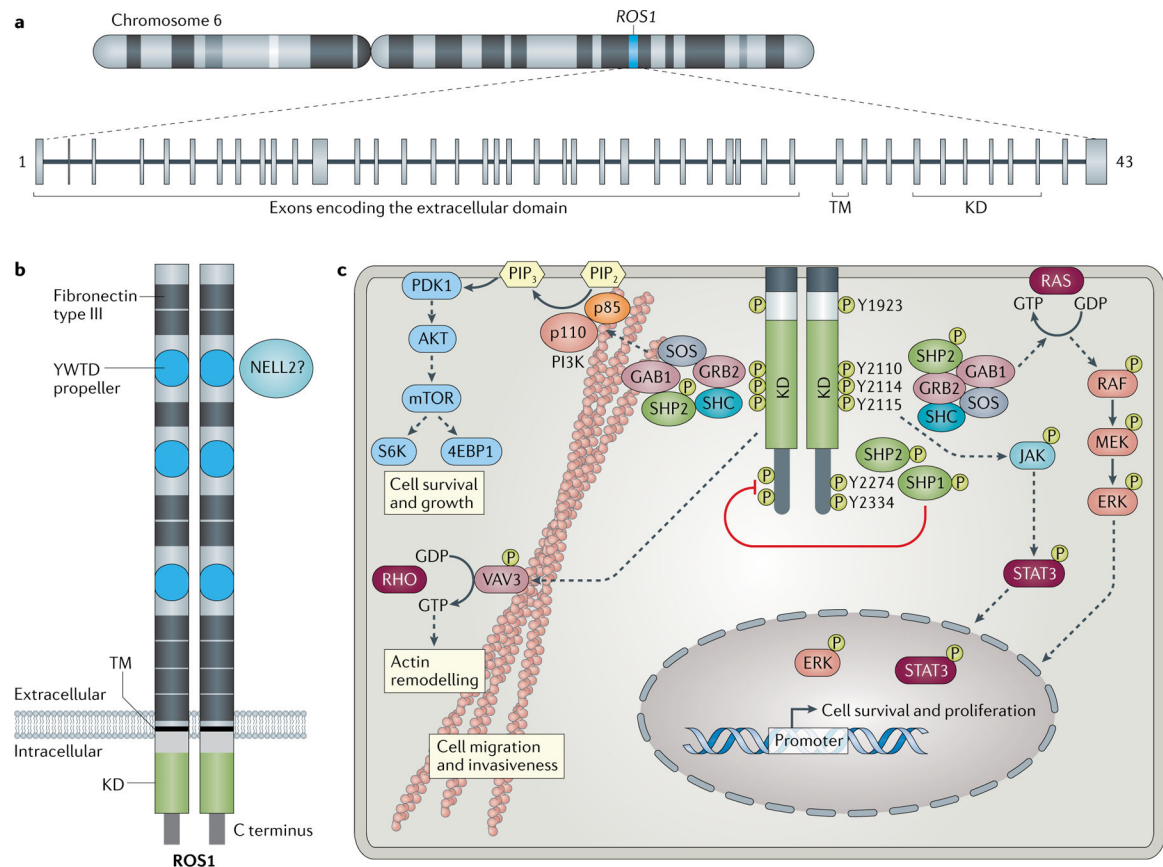


Fig. 1 | *ROS1* gene, structure and signalling.

a | *ROS1* is located on the minus strand of chromosomal region 6q22.1 (upper part), although the plus strand orientation is depicted here for simplicity and consists of 43 exons (lower part). The first 32 exons encode the extracellular region of *ROS1*, exon 33 encodes the single transmembrane (TM) domain and exons 36–41 encode the kinase domain (KD). **b** | The *ROS1* receptor domain structure, predicted on the basis of homology with other proteins, consists of nine fibronectin type III motifs, three β -propeller (YWTD repeat) domains, a single TM domain and an intracellular tyrosine KD. In mice, neural epidermal growth factor–like like 2 (NELL2) has been shown to bind with mouse *ROS1* in the epididymis and is presumed to mediate *ROS1* homodimerization (as shown) or oligomerization, resulting in activation of the KD and autophosphorylation and thus in *ROS1* signalling. Whether human NELL2 binds to the cognate *ROS1* receptor in relevant tissues, such as the human lungs or testes, currently remains unknown. **c** | Cell signalling pathways induced by *ROS1* catalytic activity include the RAS–RAF–MEK–ERK (MAPK), PI3K–AKT–mTOR, JAK–STAT3 and VAV3–RHO pathways. Autophosphorylation occurs at various tyrosine residues (Y1923, Y2110, Y2114, Y2115, Y2274 and Y2334) in the *ROS1* intracellular domain, as detected by mass spectrometry. The precise docking sites for GRB2, SHC, SOS and p110 (PI3K) have not been clearly defined; however, phosphorylated Y2274 is a known docking site for the non-receptor tyrosine phosphatases SHP2 (PTPN6) and SHP1 (PTPN11). Phosphorylation of SHP2 on the canonical Y542 and Y580 sites by *ROS1* enhances the catalytic activity of this phosphatase and facilitates the recruitment of

additional SH2 domain-containing adaptor proteins, including GRB2 and SHIP1. VAV3, a guanine exchange factor for the small G protein RHO, is recruited to and phosphorylated by ROS1, resulting in RHO-mediated actin cytoskeletal remodelling²¹⁵. These pathways induce various cellular processes that generally promote cell survival, growth, proliferation, migration and invasiveness, all of which are implicated in oncogenesis.

Author Manuscript

Author Manuscript

Author Manuscript

Author Manuscript

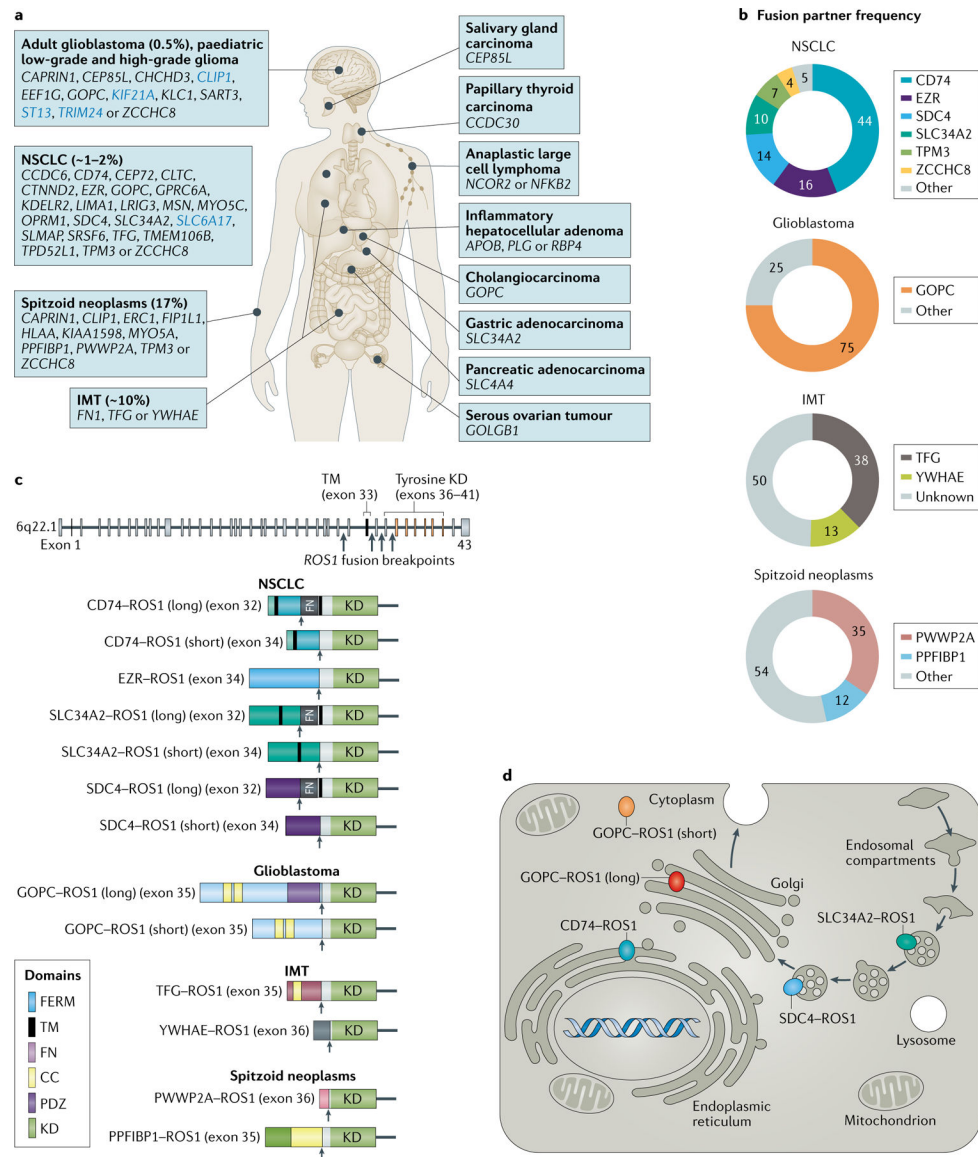


Fig. 2 | ROS1 fusion structure and cellular location.

a | *ROS1* fusions have been identified in several cancer types that occur in adults and/or children (shown on a body map). Upstream gene partners of *ROS1* fusions found in specific cancer types are listed. Among these, *CLIP1*, *KIF21A*, *ST13*, *TRIM24* and *SLC6A17* (blue font) were identified within the cBioPortal database but have not been reported in peer-reviewed publications. In terms of the absolute number of patients affected, *ROS1* fusions are most often found in non-small-cell lung cancers (NSCLCs) given the substantial global burden of this disease relative to that of other malignancies. According to data from the cBioPortal, 78% of patients found to have a *ROS1* fusion in their cancer had lung adenocarcinoma, with other cancers accounting for the remaining 22%. The prevalence of *ROS1* fusions is higher among certain rare cancers such as Spitzoid neoplasms and inflammatory myofibroblastic tumours (IMTs), which affect a smaller total number of patients as compared with NSCLC. The reported prevalence of *ROS1* fusions is indicated

for certain cancers in parentheses in the Figure. **b** | *ROS1* fusion partner frequencies in *ROS1*-rearranged NSCLCs, adult glioblastomas, IMTs and Spitzoid neoplasms are shown in circular plots (percentages shown). Large-cohort studies are lacking for other cancer types, and frequency data are thus unavailable. See Supplementary Table 1 for data on median or aggregate frequencies for each cancer type. **c** | The locations of four major intronic breakpoints (within introns 31, 33, 34 or 35) that generate *ROS1* fusions are indicated by arrows in the upper panel. The domain organization of recurrent *ROS1* fusions in NSCLC, glioblastoma, IMT and Spitz tumours is shown in the lower panel. An intact *ROS1* tyrosine kinase domain (KD) and the C-terminal domain (corresponding to exons 36–43) are included in all fusions. However, *ROS1* fusions can also include a portion of the last fibronectin type III (FN) motif repeat (exon 32), the transmembrane (TM) domain (exon 33) and/or a portion of the juxtamembrane domain (exons 34 and 35) of *ROS1*; retention of portions of these domains does not seem to affect oncogenicity. The majority of NSCLC-associated *ROS1* fusion partners lack dimerization motifs, suggesting that canonical dimerization might not be required for oncogenic activation. Distinct from the native receptor, *ROS1* fusions might be activated simply by conformational changes induced by the removal of most of the extracellular domain and redirection of this activity to novel subcellular locations. **d** | The subcellular localizations of select *ROS1* fusion proteins are depicted. CC, coiled-coil domain; FERM, band 4.1 homology and ezrin–radixin–moesin domain; PDZ, PSD95, Dlg1 and ZO-1 domain.

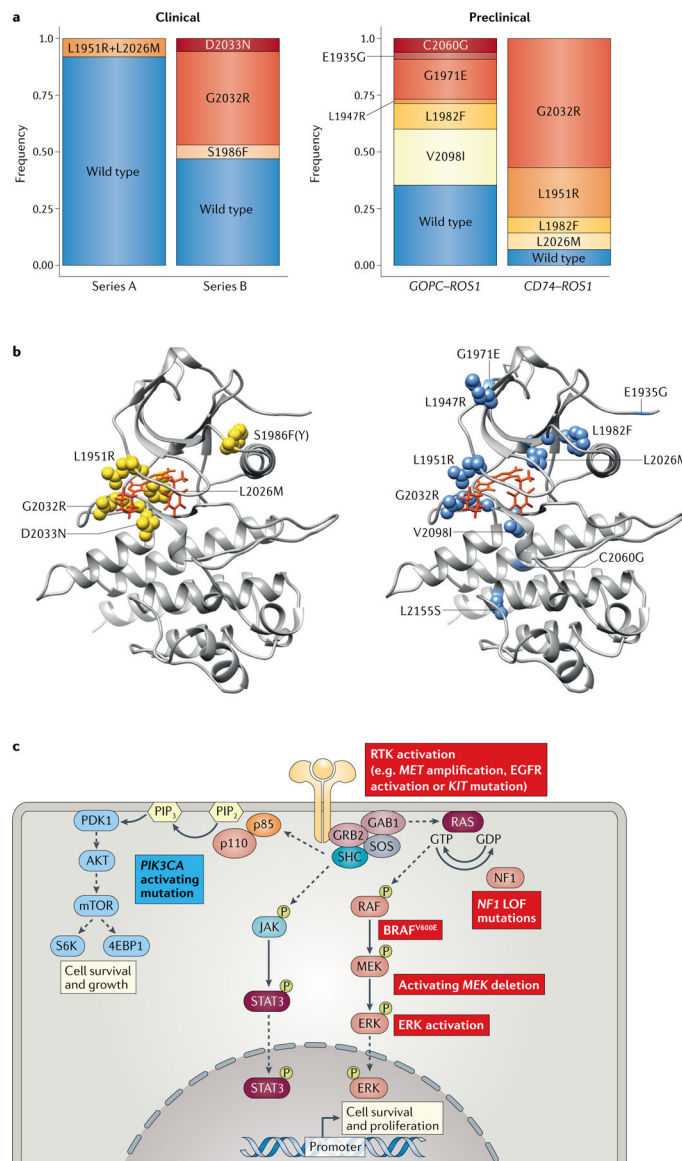


Fig. 3 | Mechanisms of resistance to ROS1 TKIs.

a | The frequencies of ROS1-intrinsic and ROS1-extrinsic crizotinib resistance observed in clinical studies^{143,170} (left) and in preclinical discovery experiments^{124,129} (right) are plotted. Data on primary resistance to ROS1 tyrosine kinase inhibitor (TKI) therapy and the precise frequency of *ROS1* mutations in patients pre-treated with TKIs are not well defined. In one series (Series A)¹⁷⁰, only 1 of 12 patients (8%) with crizotinib-resistant cancers had a detectable *ROS1* kinase domain (KD) mutation; however, in another series (Series B)¹⁴³, 9 of 17 patients (53%) had KD mutations. The overall frequency and diversity of acquired *ROS1* KD resistance mutations observed in preclinical studies is larger than those reported in clinical studies. In addition, within preclinical studies, limited overlap has been observed between the resistance mutations discovered in the context of the *GOPC-ROS1* versus *CD74-ROS1* fusions. With *CD74-ROS1*, the L1982F substitution occurred concurrently with M2128V and L2026M co-occurred with K2003I (not shown). Neither

of these two pairs of co-mutations were functionally tested for their resistance potential when engineered in *cis* as compound mutations; however, both L1982F and L2026M confer crizotinib resistance as single mutations. Additional preclinical and clinical studies are needed to ascertain whether resistance mutation profiles vary by specific *ROS1* fusion types owing to subtle conformational differences between them. **b** | The amino acid substitutions that were observed in the aforementioned clinical studies^{143,170} (left) and preclinical saturated mutagenesis experiments^{124,129} (right) are mapped onto the crystal structure of the ROS1 KD. Both S1986F and S1986Y substitutions have been reported, although only the S1986F substitution is shown. L2155S substitution (right panel) has been identified but has not been functionally validated. The ribbon diagram depicting the crystal structure of the ROS1 KD, in complex with crizotinib (orange), is adapted from PDB 3ZBF. The solvent front substitutions (G2032R, D2033N and L1951R) and other substitutions in the drug binding pocket (V2098I and L2026M) introduce steric hindrance and diminish high-affinity crizotinib binding. The reduced crizotinib affinity for S1986F/Y, L1947R, G1971E, E1935G and C2060G is either confirmed or likely to reflect other conformational changes within the kinase domain structure. **c** | Mechanisms of ROS1-extrinsic resistance include mutations and/or copy number increases involving other receptor tyrosine kinases (RTKs) or downstream MAPK pathway effectors (indicated in red), thus establishing MAPK pathway reactivation as a convergent mechanism of resistance. An activating *PI3KCA* mutation (blue) has been reported in a patient with ROS1 TKI resistance. *CTNNB1* (β -catenin) mutations have also been discovered in patients but are not shown in this figure. LOF, loss of function.

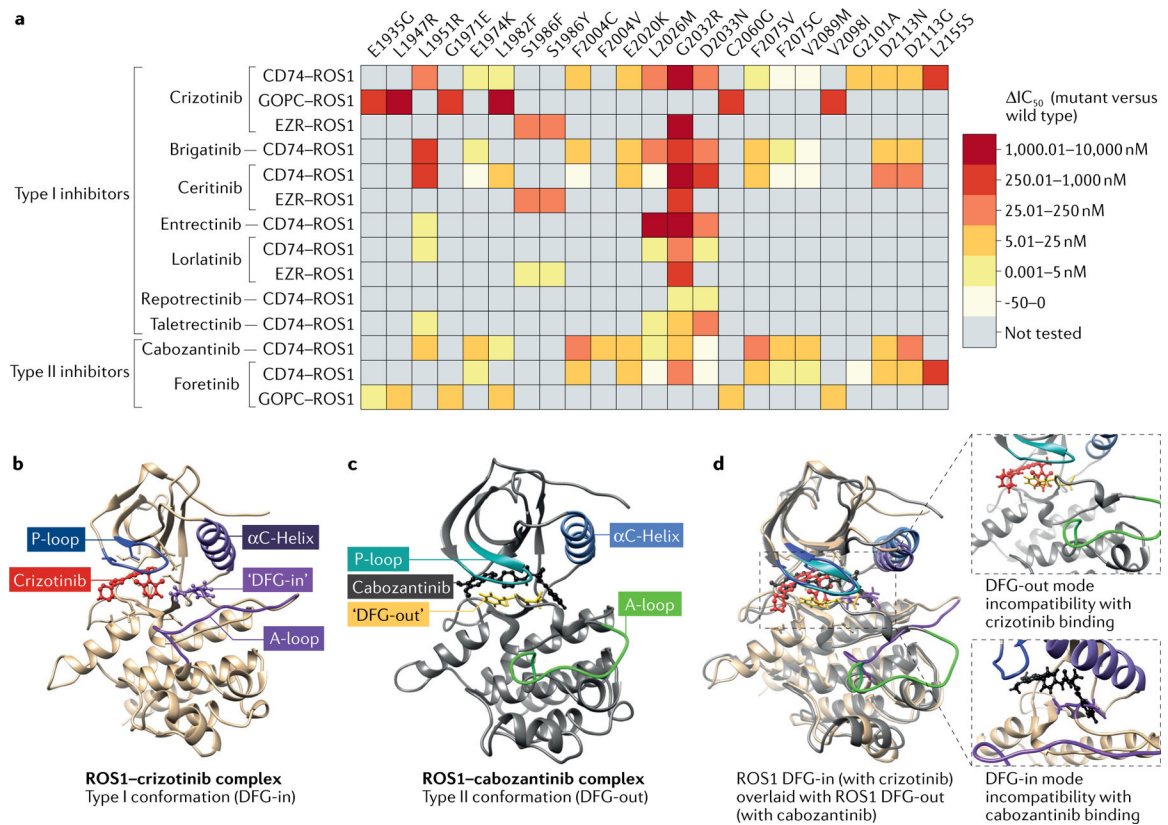


Fig. 4 | Preclinical activity and binding modes of ROS1 TKIs.

a | A heatmap comparing the activity of type I and type II ROS1 tyrosine kinase inhibitors (TKIs) against ROS1 kinase domain (KD) substitution variants. Cell-based half maximal inhibitory concentration (IC_{50}) values were obtained from eight studies that tested the activity of indicated ROS1 TKIs in CD74-ROS1-transformed Ba/F3 cells^{118–120,124,126,127,129,186} and from one study each for GOPC-ROS1-expressing⁶⁰ or EZR-ROS1-expressing Ba/F3 cells¹²⁸. IC_{50} was calculated as follows: IC_{50} (with the mutant fusion protein) – IC_{50} (with the wild-type fusion protein in the same study). Averages values of IC_{50} were taken across studies that tested the same TKI in Ba/F3 cells transformed with the same *ROS1* fusion (that is, separate averages for studies with CD74-ROS1 and those with GOPC-ROS1). Based on the correlation between preclinical inhibitory activity and the known clinical activity of a given inhibitor for the specific resistance mutation, we classified the changes in IC_{50} as follows: $IC_{50} < 5$ nM equates to a modestly altered TKI affinity but no resistance; IC_{50} of 5–25 nM equates to intermediate resistance to the TKI; and $IC_{50} > 25$ nM equates to resistance. Negative IC_{50} values indicate varying degrees of TKI sensitization to ROS1 substitutions. See Supplementary Figure 1 for comparative IC_{50} values of ROS1 inhibitors tested against different *ROS1* fusions in the Ba/F3 cell model system. **b** | Structural model showing that crizotinib (red) preferentially binds to the active, type I (aspartate-phenylalanine-glycine (DFG)-in) conformation of the ROS1 KD (adapted from PDB 3ZBF). The atoms of the DFG motif are shown in stick configuration in purple. In the type I state, the aspartate of the DFG motif is optimally positioned to bind magnesium ions and coordinate the β and γ phosphates of ATP in order to facilitate transfer

of the γ phosphate (type I inhibitors compete with ATP binding), and the phenylalanine is tucked into a hydrophobic pocket; the activation loop (A-loop, shown in purple) has an open and extended conformation. **c** | Molecular model showing ensemble docking of cabozantinib (black) to the type II (DFG-out) conformation of ROS1 KD, generated using computational chemistry as previously described^{124,127}. Atoms of the DFG residues are shown in yellow (stick configuration). In the type II conformation, the phenylalanine (of DGF) is displaced from the hydrophobic pocket, leading to reorientation of the aspartate and causing steric hindrance to ATP binding. The A-loop (green) is collapsed onto the surface of the kinase. **d** | Superimposed structures of type I and type II ROS1 KD conformations docked with crizotinib and cabozantinib, respectively, were generated using MatchMaker analysis (Chimera). Expanded views to the right show steric incompatibility within the binding pocket of the DFG-in (type I) conformation for cabozantinib (upper inset panel) and of the DFG-out (type II) conformation for crizotinib (lower inset panel).

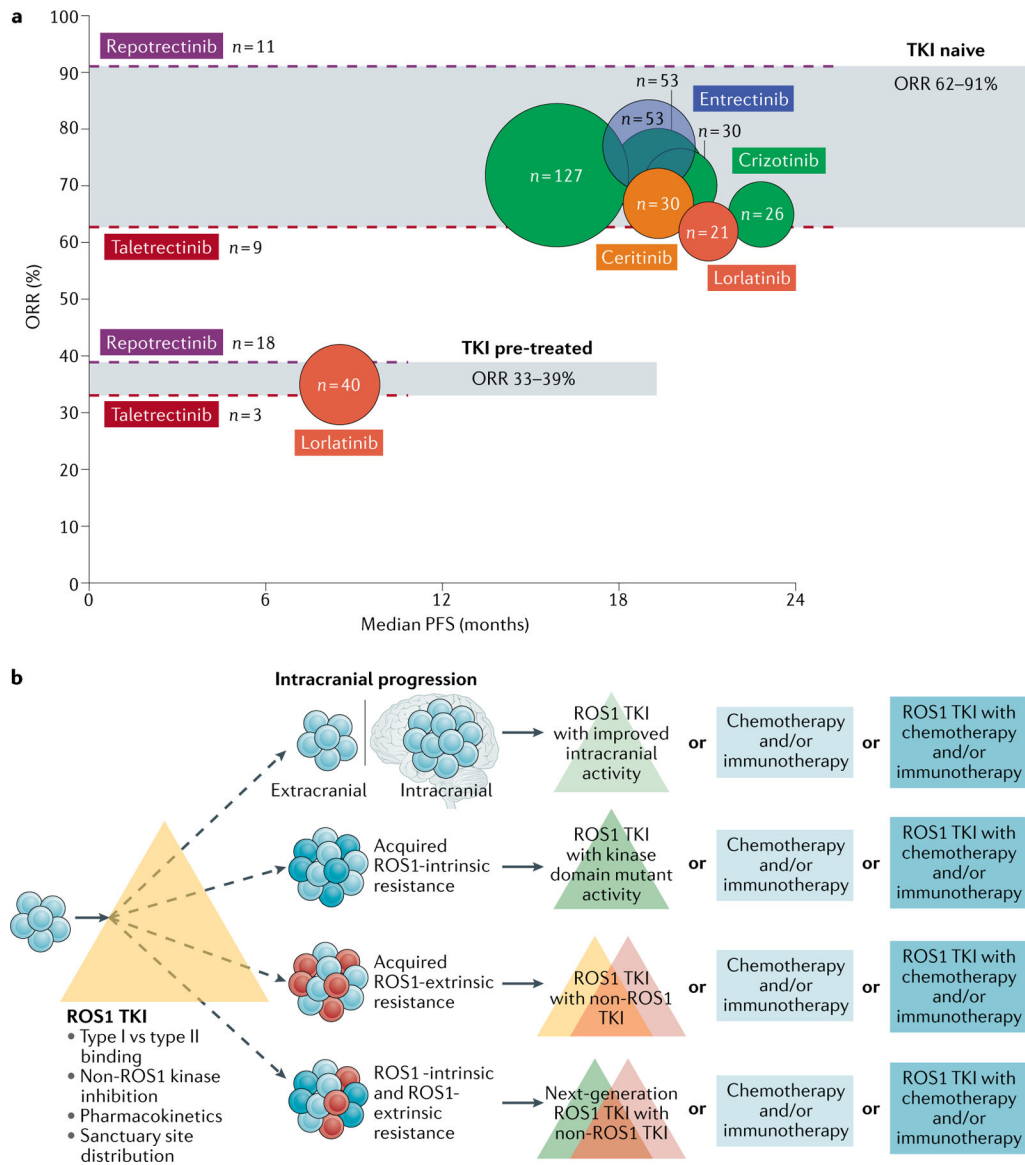


Fig. 5 |. Clinical activity of ROS1 TKIs and potential treatment algorithm for ROS1-rearranged cancers.

a | A plot summarizing the activity of various ROS1 tyrosine kinase inhibitors (TKIs) tested in prospective trials involving patients with ROS1 fusion-positive non-small-cell lung cancer (NSCLC). The activity of early-generation and next-generation TKIs is compared in terms of objective response rate (ORR) and median progression-free survival (PFS). With TKIs for which only the ORR from a single trial is known based on preliminary data and the median PFS has not been reported, a dotted line indicates the preliminary ORR. For crizotinib, four separate studies (PROFILE 1001, OxOnc, EUCROSS and METROS) are shown. One outlier trial (AcSe) that had a much lower median PFS duration (5.5 months) than all reported prospective and retrospective (TABLE 1, Supplementary Table 3) studies has been excluded; the reason for the much shorter median PFS observed is unclear.

b | A putative treatment algorithm for patients with ROS1 fusion-positive cancers. This begins with upfront ROS1 TKI therapy, which is the current standard of care for patients

with advanced-stage *ROS1*-rearranged NSCLCs. Therapeutic choices for patients who are treatment naive with other *ROS1*-rearranged cancers should reflect known and emerging data. In patients treated upfront with a *ROS1* TKI, sanctuary site distribution (for example, related to intracranial plasma concentration), other pharmacokinetic characteristics, binding mode and the spectrum of targets beyond *ROS1* present competing evolutionary pressures that vary between different TKIs. Resistance to *ROS1* TKIs can take the form of one or more of the following: sanctuary site progression, *ROS1*-intrinsic resistance (for example, a *ROS1* kinase domain mutation) or *ROS1*-extrinsic resistance (for example, bypass signalling pathway activation). The presence and degree of intratumoural and intertumoural heterogeneity in resistance mechanisms might inform therapeutic choices. Current and potential future treatment strategies include TKI generation or type switching, the administration of chemotherapy and/or immunotherapy, and the combination of a *ROS1* TKI with other types of therapy. In patients with *ROS1*-rearranged NSCLC that is resistant to an approved *ROS1* TKI, chemotherapy and/or immunotherapy is the current standard of care treatment; however, sequential TKI therapy is being explored in trials. The combination of targeted therapy with chemotherapy has yet to be explored in prospective trials. This algorithm applies only to advanced-stage cancers, and the delineation of strategies for earlier-stage *ROS1*-rearranged disease will require additional study. Indeed, the role of neoadjuvant or adjuvant therapy that includes a *ROS1* TKI has not been elucidated thus far, although this paradigm has received regulatory approval in certain other oncogene-driven cancers (for example, adjuvant dabrafenib and trametinib for *BRAF*^{V600E/K}-mutant melanomas).

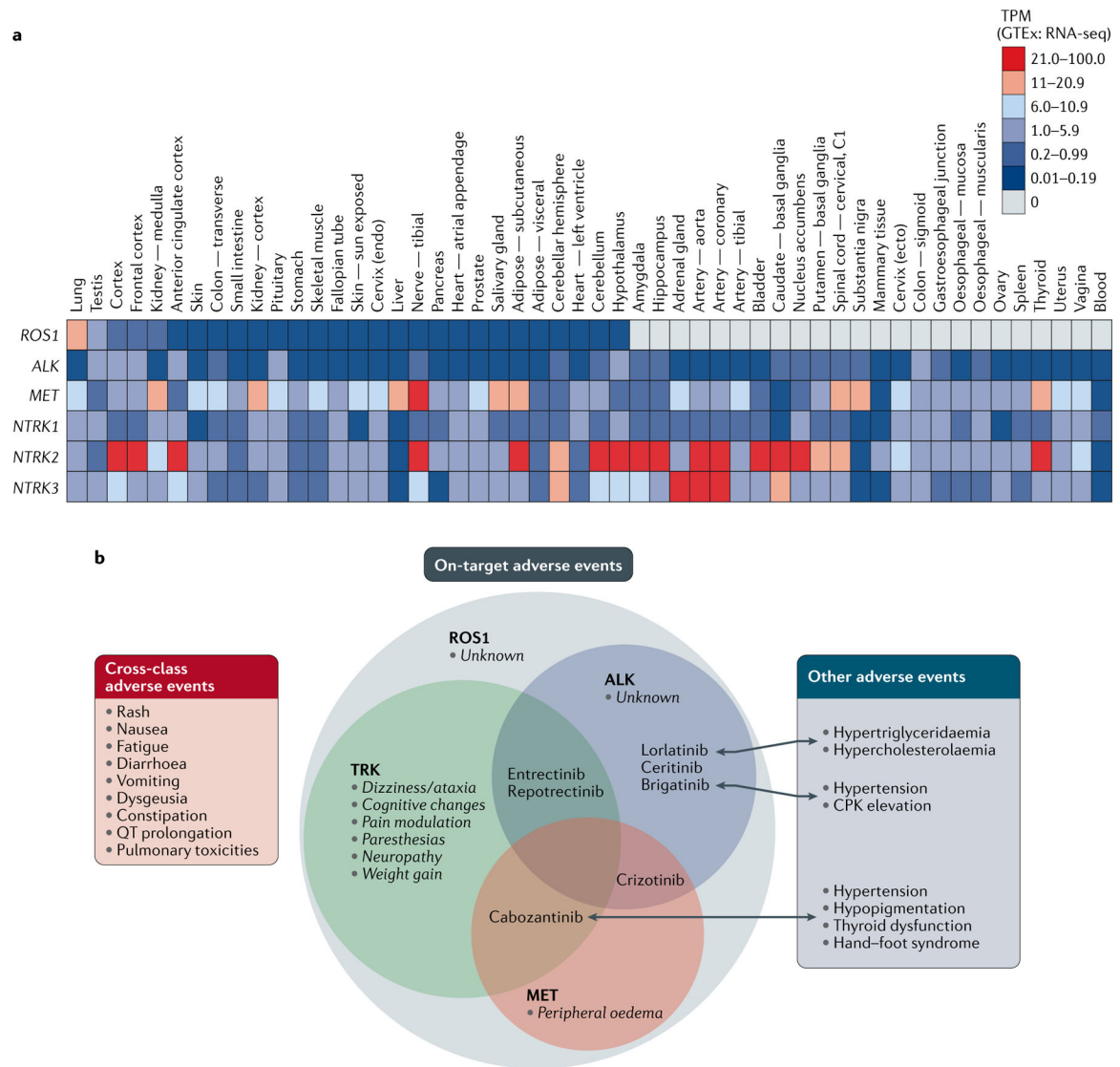


Fig. 6 | ROS1 expression and ROS1 inhibitor safety profile.

a | A heat-map of mRNA expression shows that *ROS1* is highly expressed in the human lung and, to a lesser degree, in the brain, kidney and testes. In addition to *ROS1*, levels of *ALK*, *MET*, *NTRK1*, *NTRK2* and *NTRK3* mRNA expression are shown for reference, given that all current ROS1 tyrosine kinase inhibitors (TKIs) also target one or more proteins encoded by these genes. Expression levels are shown in transcripts per million (TPM) values. These publicly available RNA sequencing (RNA-seq) data were obtained from the GTEx Portal²¹⁶.

b | A Venn diagram (centre) depicting the spectrum of kinase inhibition of several ROS1 TKIs. Some of the adverse effects of selective TRK or MET inhibitors are known, whereas the profile of toxicities that are specifically mediated by ROS1 or ALK inhibition remains largely unknown. This knowledge gap is secondary to the fact that selective ROS1 or ALK inhibitors have not been developed (current inhibitors of these kinases have multiple other targets). By contrast, selective TRK or MET TKIs and monoclonal antibodies targeting MET have been tested in clinical trials. Beyond toxicities mediated by the inhibition of TRK

or MET, adverse events observed across various TKI classes (left) and unique additional toxicities associated with certain TKIs (right) are listed.

Author Manuscript

Author Manuscript

Author Manuscript

Author Manuscript

Table 1 |

Trials of ROS1 TKIs in patients with *ROS1* fusion-positive NSCLC

ROS1 TKI	Study (phase)	Overall outcomes			Intracranial outcomes		
		ORR (n)	Median DoR	Median PFS	Median OS	ORR (n)	Other
<i>ROS1 TKI-naive setting</i>							
Crizotinib	PROFILE 1001 (REF. ¹⁴¹) (Ib)	72% (38/53)	24.7 months	19.3 months	51.4 months	–	–
	OxOne ¹⁰¹ (II)	72% (91/127)	19.7 months	15.9 months	–	–	–
	EUCROSS ²¹² (II)	70% (21/30)	19.0 months	20.0 months	–	–	–
	AcSe ²¹³ (II)	69% (25/36)	–	5.5 months	17.2 months	–	–
	METROS ¹⁶⁷ (II)	65% (17/26)	21.4 months	22.8 months	–	33% (2/6)	–
Entrectinib	Drilon et al. ¹⁴⁵ (I/II)	77% (41/53)	24.6 months	19.0 months	–	55% (11/23)	DoR 12.9 months; PFS 7.7 months
<i>ROS1 TKI-pre-treated setting</i>							
Ceritinib	Lim et al. ¹⁴⁶ (II)	67% (20/30)	21.0 months	19.3 months	24.0 months	29% (2/7)	–
Brigatinib	Gettinger et al. ²¹⁴ (I)	100% (1/1)	–	–	–	–	–
Lorlatinib	Shaw et al. ¹⁴⁷ (I/II)	62% (13/21)	25.3 months	21.0 months	–	64% (7/11)	–
Reporrectinib	Cho et al. ¹⁶⁹ (I/II)	91% (10/11)	–	–	–	100% (3/3)	–
Talrectinib	Fujiwara et al. ¹⁴⁹ (I)	67% (6/9)	–	–	–	–	–
<i>ROS1 TKI-pre-treated setting</i>							
Entrectinib (after crizotinib)	Drilon et al. ¹²³ (I/II)	0% (0/6)	–	–	–	–	–
Ceritinib (after crizotinib)	Lim et al. ¹⁴⁶ (II)	0% (0/2)	–	–	–	–	–
Brigatinib (after crizotinib)	Gettinger et al. ²¹⁴ (I)	0% (0/2)	–	–	–	–	–
Lorlatinib	Shaw et al. ¹⁴⁷ (I/II)	After crizotinib, 35% (14/40); after 2 prior TKIs: 0% (0/6)	After crizotinib: 13.8 months; after 2 prior TKIs: –	After crizotinib: 8.5 months; after 2 prior TKIs: –	–	After crizotinib: 50% (12/24); after 2 prior TKIs: 66% (2/3)	–
Reporrectinib	Drilon et al. ¹⁸⁷ (I/II)	After 1 prior TKI: 39% (7/18); after 2 prior TKIs: 29% (2/7)	–	–	–	After 1 prior TKI: 75% (3/4); after 2 prior TKIs: –	–
Talrectinib (after crizotinib)	Fujiwara et al. ¹⁴⁹ (I)	33% (1/3)	–	–	–	–	–

Author Manuscript

Author Manuscript

Author Manuscript

Author Manuscript

ROS1 TKI	Study (phase)	Overall outcomes		Median DoR	Median PFS	Median OS	Intracranial outcomes	
		ORR (n)	ORR (n)				ORR (n)	Other

The clinical outcomes of prospective early phase trials of early-generation ROS1 tyrosine kinase inhibitors (TKIs) are summarized. Outcomes with crizotinib, entrectinib and ceritinib in the ROS1 TKI-naïve setting and ceritinib in the ROS1 TKI-pre-treated setting reflect treatment at the recommended dose of each drug. The remaining trials included patients treated with a variety of doses of the ROS1 TKI during phase I dose escalation. DoR, duration of response; NSCLC, non-small-cell lung cancer; ORR, objective response rate; OS, overall survival; PFS, progression-free survival.